

LONG-TERM EFFECTS OF SYNTHETIC FIBERS  
ON CONCRETE PIPES

by

SASAN FARROKHI GOZARCHI

Presented to the Faculty of the Graduate School of  
The University of Texas at Arlington in Partial Fulfillment  
of the Requirements  
for the Degree of

MASTER OF SCIENCE IN CIVIL ENGINEERING

THE UNIVERSITY OF TEXAS AT ARLINGTON

AUGUST 2014

Copyright © by Sasan Gozarchi 2014

All Rights Reserved



### Acknowledgements

I would like to, first and foremost, thank Dr. Ali Abolmaali my research advisor, for all his support, advice and encouragement. I truly appreciate having him as my advisor and being given the opportunity to work with him. Secondly, I would like to thank my committee, Dr. Siamak Ardekani and Dr. Yeonho Park, for their time and effort while serving on my committee.

I would also like to thank Hanson Pipe and Precast for allowing me to conduct my research at their facility. Special thanks to Dr. Yeonho Park for helping me with the field work, the material needed for my research, and for coordinating my project. Also, I'd like to thank all the members of the CSER lab for their help and support, especially Margarita Takou.

Lastly but not least, I would like to extend my sincere gratitude to my parents and siblings (Ladan and Saman), for their continuous support, motivation, advice and love throughout my academic life. Without them, this would never be possible

May 12, 2014

Abstract

LONG-TERM EFFECTS OF SYNTHETIC FIBRES  
ON CONCRETE PIPES

Sasan Farrokhi Gozarchi, M.S

The University of Texas at Arlington, 2014

Supervising Professor: Ali Abolmaali

The studies undertaken by this research were to evaluate the long-term performance and durability of synthetic fiber-reinforced concrete pipes. The target long-term performance is for 9000 hours. Two sets of pipes 8 ft. (2400 mm) long with inside diameters of 24 in. (600 mm) and 36 in. (1200 mm) were manufactured, with a wall thickness of 3 and 4 in., respectively. The pipes were produced based on ASTM C76, for a Class III type with a Wall B. The two set of pipes included RCP's (as control) and SYN-FRCP's. The SYN-FRCP's had several fiber dosages ranging from 6 lb/yd<sup>3</sup> (3.5 kg/m<sup>3</sup>) to 12 lb/yd<sup>3</sup> (7.0 kg/m<sup>3</sup>) in order to evaluate the long-term performance of synthetic fiber-reinforced concrete pipes. The pipes were pre-cracked until the first visible crack was observed in the three-edge bearing test. As a result, the sustained load simulated, was calculated from the Peak D-load observed; and also the appropriate fiber dosages required for the 24. in (600 mm) and 36 in. (900 mm) pipes were obtained .Three of the 24 in. and three of the 36 in. pipes were installed in 7 ft. (2100 mm) and 8 ft. (2400 mm) wide trenches with 16 ft. (4800 mm) and 18 ft. (5500 mm) of cover respectively. The pipe was initially backfilled with native soil up to 2 ft. (600 mm) and 4 ft. (1200 mm) over the top of the pipe then backfilled again with pea-gravel weighing 100 lb/ft<sup>3</sup>, to a height of



14ft. to simulate the sustained loading. A type two installation was used during the development of the test setup.

Once the long-term test set up was complete, the data was immediately recorded, and vertical deflections were observed from the time-dependent behavior of the pipes. It was observed from results obtained from the three-edge bearing test, that synthetic fibers improve the mechanical properties of concrete pipes, in dry-cast manufacturing. Also, it was observed from the time-dependent deformation, that there was no significant deformation of SYN-FRCP, while the shear capacity was enhanced. Based on the long-term monitoring of the buried pipes, it was observed that the increase in vertical deformation of the SYN-FRCP compared to RCP, over time, was not significant.

## Table of Contents

Acknowledgements .....	iii
Abstract .....	iv
List of Illustrations .....	viii
List of Tables .....	x
Chapter 1 Introduction, Literature Review and Goals and Objectives.....	1
1.1    Introduction .....	1
1.1.1    Design of Concrete Pipe .....	3
1.1.2    Fibers in General and Properties .....	7
1.1.3    Production Locations, Manufacturing, Methods and Equipment.....	10
1.2    Literature Review.....	18
1.2.1    Fibers in General (Steel) .....	18
1.2.2    Synthetic Fiber Concrete .....	25
1.3    Goals and Objectives .....	30
Chapter 2 Field Experimental Set-Up and Monitoring .....	32
2.1    Location .....	32
2.2    Material Property .....	33
2.3    Short-Term Test – Three-edge Bearing Test .....	37
2.4    Long-Term Test – Buried Pipes.....	41
2.4.1    Detailed Construction .....	41
2.4.2    Instrumentation.....	56
2.4.3    Applied Load .....	58
2.5    Test results and Discussion.....	60
2.5.1    Short-Term Response – Three-Edge Bearing Test .....	60
2.5.2    Long-Term Response – Time-Dependent Behavior .....	65

2.5.3 Crack Width .....	69
Chapter 3 Summary and Conclusion .....	71
Appendix A Pipe Set-Up 24 in. (600 mm) and 36 in. (900 mm).....	73
References.....	92
Biographical Information .....	96

## List of Illustrations

Figure 1-1 Pipe/Installation terminology.....	2
Figure 1-2 Concrete pipe applied loads .....	3
Figure 1-3 Photograph of BASF MasterFiber MAC Matric fiber .....	10
Figure 1-4 Photograph of steel cage machine.....	12
Figure 1-5 Photograph of steel cage after production .....	12
Figure 1-6 Photograph of concrete mix with added fiber .....	13
Figure 1-7 Photograph of Packerhead equipment at Hanson facility .....	14
Figure 1-8 Photograph of three-piece jacket (metal pipe form) at Hanson facility.....	15
Figure 1-9 Photograph of the curing chamber .....	16
Figure 1-10 Photograph of the produced pipe .....	17
Figure 1-11 Photograph of BASF MasterFiber MAC FS7 fiber.....	20
Figure 1-12 Outline of this Study .....	31
Figure 2-1 Location of test set-up and monitoring .....	32
Figure 2-2 MasterFiber MAC Matrix.....	33
Figure 2-3 Typical synthetic fiber distribution.....	35
Figure 2-4 Pipe specimens produced .....	36
Figure 2-5 Schematic of three-edge bearing test .....	38
Figure 2-6 Cable displacement sensor .....	38
Figure 2-7 Pipe test set up and crack pattern 24 in. ....	39
Figure 2-8 Main-crack at invert of 24. in pipes.....	40
Figure 2-9 Pipe test set up and crack pattern 36 in. ....	40
Figure 2-10 Cracks of 36 in. pipes .....	41
Figure 2-11 Initial trench and failure .....	42
Figure 2-12 New trenches excavated .....	43

Figure 2-13 Instrumentation headquarters.....	43
Figure 2-14 Bedding preparation-step 1 .....	45
Figure 2-15 Bedding preparation-step 2 .....	46
Figure 2-16 Pipe placing and steel capping.....	48
Figure 2-17 Backfill upto ground level-step 1 .....	49
Figure 2-18 Backfill up to ground level-step 2 .....	50
Figure 2-19 Placing of concrete culvert-step 1 .....	52
Figure 2-20 Placing of concrete culvert-Step 2.....	54
Figure 2-21 Final set-up for long-term monitoring .....	55
Figure 2-22 Sensors for long-term monitoring .....	56
Figure 2-23 Installation of sensors.....	57
Figure 2-24 Schematic of overburden load.....	58
Figure 2-25 Load-deflection curves from three-edge bearing tes.....	61
Figure 2-26 Crack pattern .....	64
Figure 2-27 Time-dependent behavior for 24 in. (600 mm) pipes .....	67
Figure 2-28 Time-dependent behavior for 36 in. (900 mm) pipes .....	68
Figure 2-29 Crack propagation of the 24 in. cracked SYN-FRCP .....	70

List of Tables

Table 1-1 Coefficients for Analysis of Pipe in Standard Installation type 1 .....	6
Table 1-2 Performance characteristics of MasterFiber MAC Matrix fiber .....	9
Table 1-3 Performance characteristics of MasterFiber FS7 fiber .....	20
Table 2-1 Mechanical and Geometric Properties .....	33
Table 2-2 Standard installation and minimum compaction requirements from ACPA.....	44
Table 2-3 Test result for Three-edge bearing test .....	63
Table 2-4 Summary of measured vertical deformation up to 9000 Hours .....	66

## Chapter 1

### Introduction, Literature Review and Goals and Objectives

#### 1.1 Introduction

Concrete pipes have been around for decades. They were prominently used by the ancient Romans, in their drainage systems, to carry water. However, in those times, the materials used for making the pipes were weak in tensile strength, resulting in pipes that could not carry any water under pressure. Since that time, fibers have been added to improve fragileness of materials, and the long-term serviceability, which includes the control of cracks. Cost, weight and tensile strength are important factors to be taken into consideration when designing pipes.

The oldest pipe installation existing today is the sanitary sewer. The first one was constructed first in Mohawk, New York in 1842, and remained in operation for more than 100 years. Later on, in 1896, the French were the first to include steel-reinforcement. Because of the success of this concept of reinforcement, it was brought to the rest of the world – to America in 1905 and to Australia in 1910.

Nearly half of the underground structures invested in America are a result of sewer systems. As a result of reasonable performance over long-term periods, concrete has become the perfect choice of material used for the production of pipes in constructing sewers. Concrete's inherent qualities, such as structural performance, durability, cost, and use as effective barriers make it an ideal material. However, the tensile strength and toughness it provides are not significant. Therefore, steel reinforcement of concrete is needed to satisfy the requirements structurally. The disadvantage of concrete pipes are the corrosion of steel and other factors that shorten the service life of the concrete in sewers.

Research on fiber-reinforced concrete is setting a new platform for design, and is being developed so that more efficient concrete pipes with reduced amount of steel reinforcement may be produced. However, current designs of concrete pipes have not yet taken advantage of discrete fibers as complementary reinforcement for enhancing structural efficiency and resolving some critical performance issues.

Figure 1-1 shows the locations of the crown, invert, and spring lines, as well as the pipe/installation terminology. Under the effect of transverse bending moments, pipes behave as rectangular reinforced concrete section.

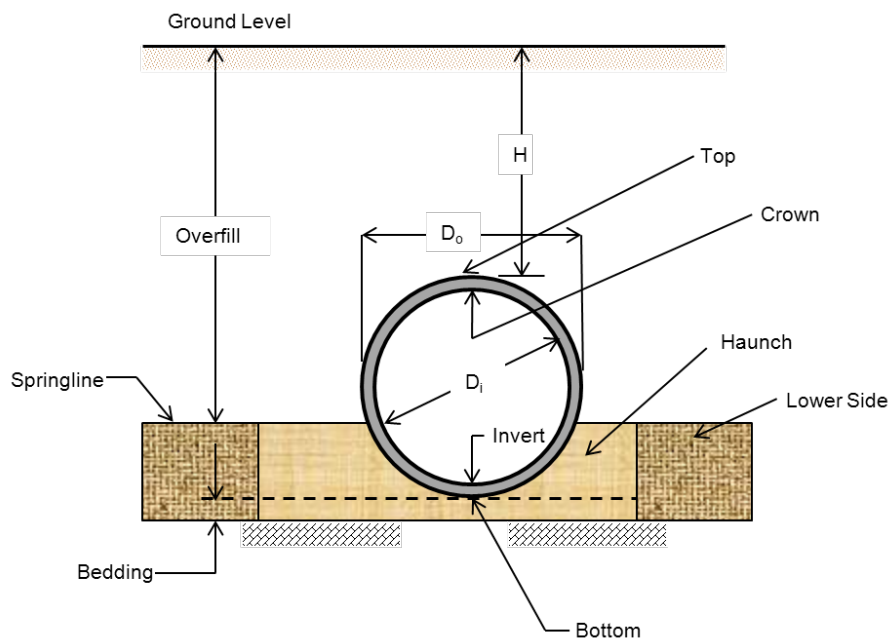


Figure 1-1 Pipe/Installation terminology

Pipes are subjected to earth pressures as shown in Figure 1.2 (a) which generates transverse bending moments in the pipe walls. Figure 1.2 (b) shows the typical steel reinforcement in concrete pipes. Figure 1.2(c) shows the flexural cracks developed under external loads, pipes first develop vertical cracks (on interior faces, crown and invert), and then horizontal cracks (at mid-heights on exterior surfaces, spring-lines).



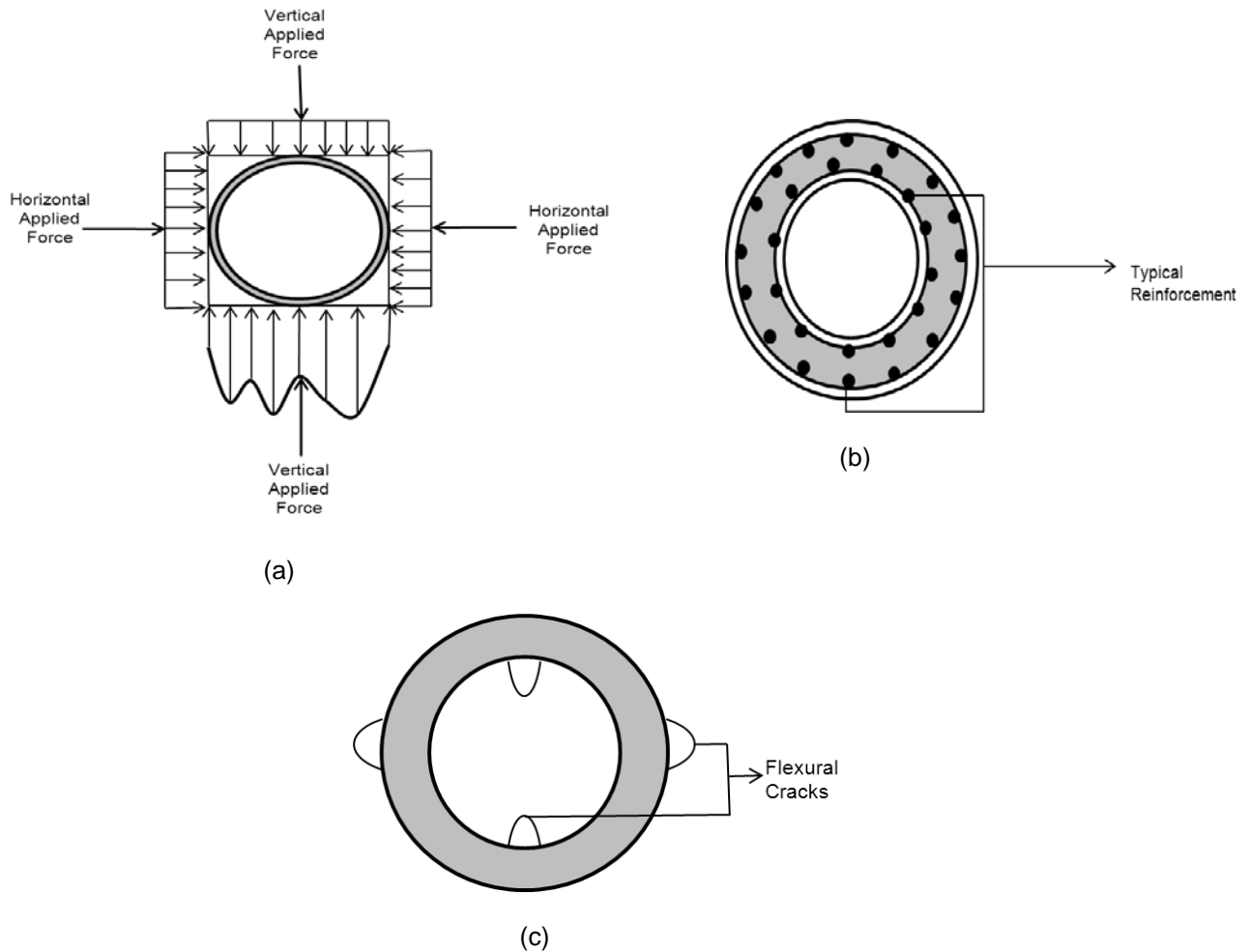


Figure 1-2 Concrete pipe applied loads: (a) vertical and horizontal loads; (b) Reinforcement system; and (c) flexural cracks

### 1.1.1 Design of Concrete Pipe

Conventionally, there are two ways in which concrete pipes are designed: direct and indirect. The main steps for designing a pipe include designing the strength of the wall needed to support the total load being applied on the pipe and determining the strength of the pipe required for support and the total load that the pipe can carry. The loads exerted on the pipe are combination of self-weight of the pipe, wheel load, earth load and surcharge load. Direct and indirect procedures use same methods in obtaining

the loads just described. Reinforcement size, reinforcement arrangement and wall thickness, together with concrete strength, contribute to the variables required to design wall thickness. The required strength of the pipe is determined by the distribution and magnitude of the load being applied to the pipe.

In the first design procedure namely, indirect design, the Marstson-Spangler procedure was used. This resulted in a bedding factor (Bf) which no longer required thrust, shear and moments acting in the pipe wall, as it describes a relationship between the total field load and the three-edge bearing load. This procedure also assumed that there was no lateral pressure acting on the side of the pipe wall, when taking into account trench condition bedding factors. On the other hand, assumption of an active lateral pressure was applied on the sides of the pipe up to the height of the natural ground for embankment conditions. This resulted in the correct bedding factor being determined, as standard installations were developed for each trench and embankment conditions. Dividing the total load by the product of the bedding factor and the diameter of the pipe gives the standard D-Load ( $D_{0.01}$ ). Multiplying  $D_{0.01}$  by a factor of safety (which is a function of the class of the pipe), gives the ultimate strength design limit ( $D_{ult}$ ). Basically, in order to design for the required strengths, indirect design procedures include results and evaluation of previous three-edge bearing tests.

The Indirect design procedure for the selection of the pipe strength includes determination of earth load and live load, determination of the bedding factor, selection of pipe strengths from the concrete design manual and selection a bedding.

The three common types of installation for this design procedure are: negative projecting embankment, positive projecting embankment and trench. The typical loads that should be included when considering buried pipes are fluid weight and internal pressure, pipe weight, earth load, surcharge loads and surface concentrated loads.

The weight of the pipe ( $W_p$ ) is insignificant compared to the other loads in most cases and can be calculated by the equations below:

$$W_p = a \times h \times (S_i + t) \quad \text{for elliptical pipes} \quad (1)$$

$$W_p = 3.3 \times h (D_i + t) \quad \text{for circular pipes} \quad (2)$$

Where,

$$a = 2.8 \quad \text{for horizontal elliptical pipes}$$

$$a = 0.2 \quad \text{for vertical elliptical pipes}$$

$D_i$  is inside diameter

$t$  is wall thickness

As for wall thickness type, wall thickness and inside diameter, the following equations describe the relation:

$$\text{Wall A: } t = \frac{D_i (in)}{12} \quad (3)$$

$$\text{Wall B: } t = \frac{D_i (in)}{12} + 1 \quad (4)$$

$$\text{Wall C: } t = \frac{D_i (in)}{12} + 1.75 \quad (5)$$

In the direct design procedure, the design of concrete pipe reinforcement is based on five limit states, namely; concrete compression, radial tension, reinforcement tension, diagonal tension and crack control. Therefore, the direct design procedure is much more flexible than the indirect design procedure.

To summarize, the direct design method uses the effects of the bending moment, shear and thrust to determine the required strength of the concrete pipe. Based on the crack width limits and strength that were developed in the long-range research program of the American Concrete Pipe Association, reinforcement design, concrete strength and wall thickness are evaluated. The moment, shear and thrust can be calculated by computer software or by hand calculations with the appropriate coefficients. The equations are as follows:

$$\text{Moment: } M_i = C_{mi} \times W_i \times \frac{D_m}{2} \quad (6)$$

$$\text{Thrust: } N_i = C_{ni} \times W_i \quad (7)$$

$$\text{Shear: } V_i = C_{vi} \times W_i \quad (8)$$

Table 1-1 Coefficients for Analysis of Pipe in Standard Installation type 1

Installation Type 1			
Location	Load Type	Coefficients	
		$C_{mi}$	$C_{ni}$
Crown	$W_p$	0.079	-0.077
	$W_e$	0.083	0.157
	$W_f$	0.057	-0.187
	$W_{L1}$	0.068	0.2
	$W_{L2}$	0.236	0.046

For pipes with diameters larger than 72 in and the D-Load greater than 2000 lb/ft/ft, the direct design method should be considered. The direct design method

equations were originally formulated for the larger diameter pipes, and therefore should be used for larger pipes to minimize reinforcement costs.

### *1.1.2 Fibers in General and Properties*

MasterFiber MAC Matrix is a synthetic fiber produced by BASF. It is manufactured in accordance with ASTM C 1116C requirements (Standard Specification for Fiber- Reinforced Concrete) made from a mix of polypropylene resins. The MasterFiber is designed primarily to compete with other fibers in the market when it comes to providing finish ability in applications such as slab-on ground and shotcrete concrete. Another main use of this fiber is as an alternative to controlling shrinkage, settlement cracking and temperature cracking. The flexural strength of concrete is greatly improved with the addition of this fiber, and provides an excellent replacement for small diameter steel reinforcement and steel fiber. Other benefits of this fiber include an increase in flexural toughness, impact resistance and shatter resistance which as a whole improve the long-term durability of concrete.

A brief list of applications, features, benefits, engineering specifications of MasterFiber MAC synthetic fiber, and performance characteristics (shown in Table 1-2), courtesy of the BASF website, are as follows:

#### Application:

- Thin-wall precast
- Pavements
- Precast Concrete
- Wall system
- Shotcrete

- Industrial and warehouse floors

Features:

- Exceptional flexural performance
- Exceptional finish ability

Benefits:

- Effective tight crack control
- Reduction in labor and production time
- Perfect control of settlement cracking
- No need of welded-wire reinforcement and small diameter bars used as additional reinforcement.
- Easily transported and handled.

Engineering Specifications:

- Enhanced cohesion
- Enhanced flexural toughness
- Enhanced shatter and impact resistance
- Better residual strength
- Better durability
- Reduced rebound
- Used as a replacement of other secondary reinforcement and welded wire reinforcement

Table 1-2 Performance characteristics of MasterFiber MAC Matrix fiber

Physical Properties	
Configuration	Stick – Like fiber
Fiber Type	Embossed
Material	100% Virgin Polypropylene
Specific Gravity	0.91
Melting Point	320°F (160 °C)
Ignition Point	1094°F (590 °C)
Available Lengths	1.9 in. and 2.1 in. (48 mm and 54 mm)
Water Absorption	NIL
Tensile Strength	85 ksi (585 MPa)
Alkali Resistance	Excellent
Chemical Resistance	Excellent
Color	White, Translucent
Electrical Conductivity	Low



Figure 1-3 Photograph of BASF MasterFiber MAC Matric Fiber (Courtesy of:

<http://www.concreteconstruction.net/products/basf-corp.aspx>)

### 1.1.3 *Production Locations, Manufacturing, Methods and Equipment*

Pipes used in this study were produced and tested at Hanson Pipe and Precast Plant, located in Grand Prairie.

Materials used for manufacturing concrete pipes included, coarse aggregates, fine aggregates, Portland cement, steel reinforcements, and water. They were mixed and combined in a way that accounted for proportions and quantity. The fine and course aggregates were mixed together and then, later, with water to make a concrete mix that could be used to form pipes using different methods: Packerhead, Dry Cast and Wet Cast. Once this was done, the pipes casted were cured and moved to a storage area where they were ready to be delivered to the site needed for installation. Basically, the manufacturing process includes the following processes:



- Storage of materials
- Handling of materials
- Fabrication of cage reinforcement
- Mixing and batching of concrete
- Pipe Production
- Curing
- Yarding and Storage

#### Storage of Materials:

Aggregates are mostly stored in bins, and Portland cement and Pozzolans are kept in water tight silos. Steel reinforcements are kept near the steel fabrication area.

#### Handling of materials:

The aggregates and cement were transferred from the storage bins and silo's to weighing machines by loading the equipment using conveyer belts. The weighing bins and conveyor belts were controlled electronically by an automated process. After being weighed, the aggregates and cement were mixed and combined, and water was added to form a batch. It was now ready for the next process, pipe formation.

#### Fabrication of Reinforcement:

Cage machines lined steel wires and positioned the longitudinal wires while wrapping the circumferential wires in a spiral, in order to form the shape of the pipe. The intersection of the longitudinal wires and circumferential wires cause an automatic weld, hence a reinforced cage is produced.



Figure 1-4 Photograph of steel cage machine (Courtesy of:  
<http://www.ecvv.com/product/4032604.html>)



Figure 1-5 Photograph of steel cage after production (Courtesy of:  
<http://www.langleyconcretegroup.com/uploads/images/tour/Mastematic%20-%20Automated%20pipe%20production/8---The-pallet-automation-moves-the-pallets-forward-where-the-reinforcing-cage-is-placed-on-the-pallet,-where-needed..jpg>)

#### Batching and Mixing of Concrete:

This is the process in which the aggregates and cement, and any other admixtures used were all mixed and blended together. An example of an admixture can be fibers. Fibers were added to the mixture before water was added, to ensure even distribution throughout the mixture. Drum and pan mixers are the two most popular mixers used in the concrete pipe manufacturing industry. Figure 1.6 below shows a typical mixture of the aggregates together with the fiber added.



Figure 1-6 Photograph of concrete Mix with Added Fiber

#### Pipe Production Methods:

There are several ways in which concrete pipes are manufactured, namely Dry cast, Wet Cast and Packerhead processes, which are further explained in detail below:

##### Dry Cast Process:

This method involves using a zero slump mixture. The mix is placed in a form that is instantly set up and removed, and can be re-used several times for other pipes

being produced, using the same form work. The form work is stripped immediately when the consolidation process is complete, and the newly formed pipe can now support itself standing. In this process, low-frequency high amplitude vibrations are used in distributing and compacting the mixture, hence, ensuring a denser and durable concrete

**Wet Cast Process:**

An inner and outer form is required that uses a higher slump wet mix, which is placed in the forms. The forms cannot be removed until they are safe to handle and until the concrete pipes are have consolidated enough to achieve the desired strength to be able to stand by themselves.

**Packerhead Process:**

This process uses a three-piece jacket or metal pipe forms that are placed on a rotating floor as shown in Figure 1.7 and Figure 1.8 below:



Figure 1-7 Photograph of Packerhead Equipment at Hanson Facility



Figure 1-8 Photograph of Three-piece Jacket (metal pipe form) at Hanson Facility

After placing the three-piece jacket on the rotating floor by using a forklift, the concrete mix is carried from the conveyor belts and deposited at the discharge end of the Packherhead machine. Here, the floor rotates so as to place the metal forms in the right position for casting. This entire process is controlled by an operator that stands above on the platform, overlooking the forms, in order to control the speed of the rollers as shown on Figure 1-7 (previous page). The packer head has a rotating head which works at a high-rate speed, and forms the interior surface of the pipe. The inside diameter of the pipe is created by the spinning of the rollers, which as a result, cause concrete by radial compaction to be formed in the outer edges. As the head goes in and out of the pipe, the rollers on top of it compact the mix. As soon as the pipe is fully formed and casted, the rotating floor moves to the next empty metal jacket where the process continues. The



compacted and casted pipe, still with the form work, is moved by using a forklift to the curing kiln. The form work is disassembled and quickly taken back to the production section.

#### Curing:

Immediately after the pipe is formed, the curing process begins. The rate of hydration of cement greatly affects the curing rate. Using low pressure steam is the most common way of curing in the pipe industry. The low pressure steam accelerates the rate of hydration in concrete pipes, and hence, the required strength is reached in a shorter period of time. The most critical factors in concrete pipe curing are time, temperate and moisture. Higher temperatures would result in reduced curing time. Also, in the curing area, steam curing curtains are used and cover the newly casted pipes for some hours. This enclosed area ensures the circulation of steam around the entire pipe, as the low-pressure steam at high humidity and high temperature, are most effective in this environment. Figure 1.9 below shows the Curing Chamber.



Figure 1-9 Photograph of the Curing Chamber

Yarding and Storage:

A final visual inspection is done to ensure that all requirements have been met. In case of some slight imperfection, repairs are done before the pipes are yarded. Markings, usually by spray paint, are done on the pipe which includes pipe diameter, date manufactured, strength and fiber dosages used, if any. This is depicted in the following Figure 1-10 below.



(a)



(b)

Figure 1-10 Photograph of the produced pipe (a) Required Markings, (b) Pipes Stacked in Yards Ready for Transportation, (Courtesy of:

<http://forums.nasioc.com/forums/showthread.php?t=1008399&page=67>)

## 1.2 Literature Review

### 1.2.1 *Fibers in General (Steel)*

A brief description of steel fibers along with mechanical properties is as follows:

MasterFiber FS7 is another type of fiber that is produced by, BASF. It is made from low carbon steel that has been drawn into thin wires for reinforcement purposes. The ends of the fiber are drawn so that maximum adhesion is acquired between the concrete and the steel fibers. Basically, the fiber acts as a mechanism whereby it re-distributes the stresses that are in concrete, and hence, controls crack formation and crack extension from spreading. As a result, this enables more ductility within the reinforced concrete, thus during the post-cracking phase, the load-carrying capacity is maintained.

A brief list of applications, features, benefits, and engineering Specifications of MasterFiber MAC synthetic fibers, and the performance characteristics (shown in table 1-3), courtesy of the BASF website, are as follows:

Applications:

- Shotcrete
- Wall systems
- Concrete pavements
- Irrigation channels
- Thin-wall Precast
- Industrial and warehouse floors

Features:

- Deformed ends, mechanically
- Balling issues avoided due to loose fiber ends



Benefits:

- Enhanced flexural resistance and toughness
- Greater shear resistance and tensile strength
- Greater safety
- Enhanced Impact resistance
- Reduced cracks, hence better aesthetics
- Variable loads can be withstand
- Reduction of concrete thickness
- Faster production of pipes due to elimination of steel cage reinforcements

Engineering Specifications:

Requirements of the ASTM A 820 which is the Standard Specification for Steel Fibers reinforced concrete is met for MasterFiber FS7 BASF steel fibers. The additional international standards listed below are also met:

- UNI-EN 10016
- UNI-11037
- EN 14889

Table 1-3 Performance characteristics of MasterFiber FS7 fiber

Nominal Dimensions	
Diameter	0.0222 in. (0.55 mm)
Length	1.30 in. (33 mm)
Aspect ratio	65
Quantity of Fibers	7370 units/lb (16248 units/kg)
Mechanical Properties	
Tensile Strength	> 160 000 psi (1100 MPa)
$\Delta l$ (Strain at Failure)	< 4%



Figure 1-11 Photograph of BASF MasterFiber MAC FS7 Fiber ([Courtesy of: http://www.maccaferribalkans.com/al/category/products/](http://www.maccaferribalkans.com/al/category/products/))

Previous studies done on steel fibers are:

Ramaswamy and Thomas (2007), studied the material properties of concrete reinforced with steel fibers to determine their post-cracking response, Poisson's ratio, modulus of rupture, modulus of elasticity, strain, tensile strength and compressive strength. The steel fibers were produced at a volume fraction of 1.5% and at strengths of 35 MPa (5.08 ksi), 65 MPa (9.43 ksi) and 85 (12.33 ksi). Results of the compressive strength increased for all three concrete strengths (normal, moderately high-strength and high strength). The modulus of rupture increased by 46.2%, 38.8% and 40.0% for normal, moderately high-strength, and high-strength concrete, respectively. Modulus of elasticity increased by a small percentage of 8.3%, 9.2% and 8.2% for normal, moderately high-strength concrete and high-strength concrete, respectively. The Poisson's ratio was reported to be between 0.18% and 0.22% thus not a significant change was noted among the three types of concrete strengths. For the split tensile strength, a higher increase was observed: 38.2%, 41.2% and 38.5% for normal, moderately high-strength concrete and high strength concrete. The strain, showed an increase in value of 29.5%, 29.4% and 27.0% for normal, moderately high-strength concrete, and high strength concrete respectively. The study concluded that increasing the steel dosage would increase the post cracking reaction.

The concept of replacing the traditional steel cage reinforcement by steel fibers in large diameter pipes was carried out by Robert Henry (1974). This study showed that  $D_{0.01}$  and  $D_{ultimate}$  were passed for the 60 in. pipes that had a higher dosage of fiber. However, lower dosages of the same pipe size did not manage to pass the  $D_{0.01}$  requirements, but passed the  $D_{ultimate}$ . As for the 60 in pipes, the higher percent by volume ratios which were between 0.8% and 1.08% passed ASTM C76  $D_{0.01}$  and  $D_{ultimate}$

requirements. The study further showed that for the 54 in. diameter pipes, neither did the  $D_{0.01}$  or  $D_{ultimate}$  met the requirements, regardless of the fiber dosages used. As for the lower dosages of fiber, the  $D_{0.01}$  did not pass; consequently the  $D_{ultimate}$  requirements were not met. The study showed that steel fiber used instead of regular steel cage reinforcement was not effective unless the dosage of fiber was really high and thicker walls of pipes were used.

Swamy and Kent (1974), conducted a study on steel fibers used in concrete pipes and deck slabs. Tests were conducted on concrete pipes with varying diameter sizes. The study showed that, the ultimate load and proof load were satisfied, as required by the British Standards, BSS 556. For the deck slab test, had two slabs which were square in shape with two different thicknesses, and varying fiber dosages were used. The slabs were subjected to a point load, whereby the required load was loaded twice. It was observed that the two slabs passed the load recovery tests and no signs of cracks were seen under working load stresses.

A study conducted by Shende and Pande (2011), researched and conducted experiments regarding flexural and deflection comparisons of steel reinforced concrete beams. Three steel fibers aspect ratios of, 50, 60 and 67 were used. Fiber dosages used were 0%, 1%, 2% and 3% by volume. However, the concrete mixture was kept constant. The results of the tests showed that with the addition of steel fibers, the flexural strength increased compared to plain concrete by 8.80 MPa (1.28Ksi) - 10.40 MPa (1.51ksi), 8.40(1.22ksi) - 10.00 MPa (1.45ksi), and 8.27MPa (1.20ksi) - 9.73 MPa (1.41ksi) for 1%, 2% and 3% respectively for volume of steel fibers. This change in flexural strength is due to the change and increase in the aspect ratio. Also, it was seen that deflection curves followed a similar pattern for the fiber ratio and dosages used, with a clear reduction of steel reinforcement of about 3% in volume.

The addition of Steel fibers to wet and dry cast concrete pipes were studied and tests were carried out by MacDonald and Transgrud (2004). It was observed from the tests the fiber dosage and type greatly influence the overall strength of the pipe. The tests that provided this information were: Compressive strength, average residual strength, and the three-edge bearing test. The fiber dosages used were 0.25%, 0.50% and 0.75% per volume. Apart from the tests conducted above, the pipes were tested for ultimate load, the first 0.25mm crack and the first hairline crack. The ultimate load was compared to steel fiber reinforcement, fabric reinforcement and a combination of the two. The study concluded that, fiber steel reinforcement helps with the strength of the pipes, but is dependent upon correct dosage and application.

Cunha, Barros and Sena-Cruz (2010), studied the pullout behavior of steel fibers. In order to determine the load-slip curve, relationship between embedded length and inclination angle, and failure modes, a single hooked end type and one straight type of steel fiber were introduced into a self- compacting concrete. From the results, it was obvious that a complete pullout was the most common type of failure seen in both types of fibers. As a result of the failure governing, the hook of the bent fibers straightened out due to debonding with concrete. For aligned straight fibers, as peak load was reached, a significant load drop was seen from the load-slip curves. Rupture was the most common type of failure for inclined fibers. It was noted that the load continued to decrease as the slip increased. Fibers acted like a straight fiber after a slip for length of the hook due to the hooked fibers having less of an abrupt decrease. The study concluded that, the embedded length had very little effect on the inclined fibers and a large effect on the pullout of the aligned fibers. Finally, it was also observed that the peak load was observed to increase to an angle of about 30 degrees, then decrease from 30 to 60 degrees, in angle.

A study conducted by Abolmaali et al.(2012), showed performance of steel fiber reinforced concrete pipes. The authors compared steel fiber reinforced concrete pipes to regular reinforced concrete pipes, and several tests were undertaken in order to achieve the goals and objectives. Different production sites were selected for diversity purposes, whereby the conditions and mix design were kept constant in order to have a fair result. Pipes with various diameters ranging from 15 in. (400 mm) to 48 in. (1200 mm) and with different fiber dosages were tested. The study showed that steel reinforced concrete pipes are adequate in stiffness, strength and ability to tolerate large crack widths. Also, regardless of the pipe size, a singly unique crack was observed on the crown, invert and spring-lines. Steel fiber- reinforced pipes do not undergo any shear or debonding failure, unlike regular reinforced concrete pipes. The study concluded that, fibers with steel reinforcement take large deformations and have crack width that may be greater than ½ in. (13 mm) without crumpling, but in general, have a smaller crack width as compared to regular reinforced concrete pipe. Also, under the sustained load, the fibers failed mostly due to fracture by yielding, as opposed to pull out. Lastly, the result of the load-deformation graphs for steel fiber reinforced concrete revealed that, stiffness declines with a negative slope, then increases to zero and remains constant, unlike that of steel fiber reinforced concrete.

Mikhaylova (2013), studied and investigated steel fiber performances in reinforced concrete pipes, with the goal of being to develop material model used in dry-cast applications. This was a very in-depth study and included finite element modeling. The load-deformation graphs were obtained from the three-edge bearing test, and the overall performance of the pipe was determined. Joint shear tests and hydrostatic joint tests were undertaken in order to investigate the performance of joints in the fiber pipes, for differential displacements and water tightness. Using FEM analysis, a three-

dimensional non-linear finite element model was developed to find out material properties of the composite system of the fiber and concrete. The study concluded that steel fibers have enough strength, and stiffness to withstand large cracks without pullout, and take large deformation under the three-edge bearing test with cracks greater than ½ in. (13 mm) without collapse. As a result of the authors study and investigation, there has been approval, in the year 2013 for a stand-alone performance based specification, ASTM C1765-1, for steel fiber reinforced concrete pipes.

### *1.2.2 Synthetic Fiber Concrete*

Previous studies done on Synthetic fibers are:

An Investigation carried out by Kurtz and Balaguru (2000), on nylon and polypropylene fibers with dosages of 1.5 lb/yd<sup>3</sup>, by performing experimental programs that included post crack load-deflection behavior, time-dependent post-crack load-deflection behavior tests, and compressive strength tests. The results obtained concluded that both nylon and polypropylene fibers can resist small percentages of post crack load. Also, the net creep deformation was not that different in the two fibers. However, it was observed that nylon would creep faster and less often than polypropylene fibers.

A study conducted by Atis et al. (2009), researched the flexural and abrasion, compressive resistance of varying steel, synthetic and fly ash quantities in reinforced fiber concrete. Different volume ratios were used for the steel and synthetic fibers, ranging from 0.5% - 1.5%. The results showed that for the polypropylene fibers, when used in either plain or fly ash concrete, there was no effect in abrasion resistance.

However, in the case of steel fibers, the abrasion resistance and flexural strength were seen to increase, but the compressive strength was noted to have no change.

Alhozaimy et al. (1996), carried out a study on polypropylene fiber-reinforced concrete, with very low volume fractions of about 0.3%. The study was comprised of finding the effects of polypropylene fibers with respect to the compressive strength, flexural strength and impact resistance. The results obtained showed that for the volume fraction used, Polypropylene has little/insignificant effect on the compressive strength of the concrete and toughness. However, at 95% level of confidence, the fibers did have an effect on the toughness. It was found that flexural strengths were not affected by the addition of polypropylene fibers. The impact resistance showed that the impact resistance was greatly affected, as it increased the first crack failure. Basically, the study concluded that the addition of polypropylene fibers (for the dosages used) would increase first crack, failure impact resistance and flexural toughness. However, the addition of fiber had no effect on flexural strengths, toughness and compressive strength.

Song et al. (2005), carried out a study on nylon and polypropylene fibers reinforced concrete as compared to plain concrete at fiber content of 0.037 lb/ft<sup>3</sup> (0.6 kg/m<sup>3</sup>). The results showed an improvement in the compressive and splitting tensile strengths and the modulus of rupture in nylon fiber reinforced concrete, in comparison with the polypropylene fiber reinforced concrete. Also, the nylon fiber showed an improvement on impact resistance, the first crack and failure strength as compared to the other materials being tested, polypropylene fiber reinforced concrete. From these results obtained, the nylon fiber performed better than its counterpart, polypropylene. However, the overall performances of the two types of fiber were better in terms of material properties as compared to plain concrete.



Wang (2005), studied the effects of Aramid (short) fibers with regards to fracture and toughening of epoxy. The addition of fibers resulted in the increase of fracture resistance ( $K_{Ic}$ ). It was noted that the Aramid fibers had a toughening effect. The results of the study also showed the fracture surfaces and crack tip damage zones, from fiber pullout, fiber breakage and are the most likely reasons for the increase in fracture resistance,  $K_{Ic}$ . Another factor that contributed greatly toward the improvement of fracture toughness is the matrix shearing and tearing.

Roesler et al. (2004), studied steel and synthetic fibers under monotonic loading and compared them to plain concrete. The test results showed that, for volume fraction percentages of less than 2%, the flexural strengths test did not show much difference from plain concrete. The ultimate load increased with the addition of steel fiber as compared to synthetic and plain concrete.

A study carried out by Peyvandi et al. (2014), developed new structural equation designs and did further verification by performing experiments on concrete pipes. The new equations use synthetic fibers in order to reduce the steel ratio used for reinforcement, thus, increasing the cover of concrete on steel which results in better durability. Toughness and damage resistance of pipes are also improved with these new sets of equations developed for design. The tests that were undertaken to verify the new design equations were flexural strengths and load carrying capacity. The study concluded that depending on the load-bearing requirements, the addition of synthetic fibers can reduce the steel reinforcement in concrete pipes by 50%.

Wilson (2012), studied the performance of steel fibers and BASF synthetic fibers as a replacement to the conventional steel reinforcement. A total of 93 synthetic fibers and 60 steel fiber reinforced pipes were produced and tested to accomplish the study in

accordance with ASTM C497. Load- deformation plots for both steel and synthetic pipes were developed and studied and compared with each other and a control pipe (regular steel reinforced concrete pipe). From the plots, the different fiber dosages were compared, and the area under the curve was calculated as well as the modulus of toughness. For both the synthetic and steel fibers, when the pipe was at extreme deflection, that is, over 10% of pipe diameter, the fibers were able to resist crack widths of up to 1.0 in. The study concluded that the use of BASF synthetic fibers and steel fibers can very well act as a replacement for the conventional steel reinforcement used in pipes.

Mohammadagha (2013), studied the effects of a mixture of materials in reinforced concrete pipes with regards to improving the ductility of regular concrete pipes and thin-walled semi-rigid concrete pipes. The different concrete mixtures studied were steel bar reinforced concrete pipes, synthetic fibers, crumb rubber and steel reinforced concrete pipes. In the research, crumbed rubber replaced 3% - 20% by volume of the sand used in concrete mixture. For the 24 in. pipes tested consisting of 10pcy steel fiber and 8% crumb rubber. Steel fibers yielded and not pulled out after the first crack, showed a significant reduction in stiffness compared to the conventional concrete pipe. Also, the results showed the comparison of crack between the regular concrete pipes, thin-walled pipes and synthetic fiber pipes to have similarities. The behavior of thin-walled with crumb rubber is similar to that of thin-walled steel or synthetic fiber. The most common failure observed and noted in the 24 in. and 36 in. concrete pipes were a shear crack which occurred in the crown and invert of the pipe, vertically. But, in larger diameter pipes, the failure most frequently was due to flexural failure. The author concluded that, TW pipes, and reinforced concrete pipes have the same effectiveness when ductility is considered.

Wilson and Abolmaali (2013), carried out an investigation, comparing the material behavior of steel and synthetic fibers of zero-slump, dry-cast reinforced concrete. Various fiber dosages for both steel and synthetic fibers were used, and both flexural beam tests and compressive cylinder tests were conducted. From the test results, further studies were taken to find out the compressive strength, first-peak load, peak load, modulus of rupture and specimen toughness, in order to find the material properties. A beam-load deformation graph was also drawn for each fiber to illustrate the behavior of the fiber with its strength after the first crack. From the flexural beam test, it was determined that the both steel and synthetic fibers showed a drop in load after the first crack and first-peak load, when low dosages were used. When higher dosages were used, the beams could resist additional loads as a result of the first crack, due to strain hardening after a small drop in load. As for the steel fiber, the higher the fiber dosage, the more the beam behaved like a metallic behavior. Both modulus of rupture and the compressive strength were improved with the addition of fibers. The spreading and formation of cracks at higher dosages of fiber were similar in the two fibers, with the crack becoming more of a ductile shear type. The study concluded that, both steel and synthetic fibers were acceptable and reasonable alternatives to regular steel reinforcement used in concrete pipes, as both ductility and durability were greatly improved, with the addition of fibers.

### 1.3 Goals and Objectives

The objectives of this study are to evaluate the long-term performance and durability of synthetic fiber reinforced concrete pipes. The target long-term performance is for 9000 hours. To accomplish the above goals, the following tasks will be at the forefronts:

Two sets of pipes 8 ft. (2400 mm) long, with inside diameters of 24 in. (600 mm) and 36 in. (1200 mm) were installed, with wall thickness of 3 and 4 in. respectively. In order to evaluate the long-term performance of synthetic fiber-reinforced concrete pipes, the pipes were pre-cracked until the first visible crack was observed in the three-edge bearing test. Three of the 24 in. and three of the 36 in. pipes were installed in 7 ft. (2100 mm) and 8 ft. (2400 mm) wide trenches with 16 ft. (4800 mm) and 18 ft. (5500 mm) of cover, respectively. The pipes were initially backfilled with native soil up to 2 ft. (600 mm) and 4 ft. (1200 mm) over the top of the pipes then backfilled again with pea-gravel weighing 110 lb/ft<sup>3</sup>, to a height of 14 ft. in order to simulate the sustained loading. A type two installation was used during the development of the test setup.

Figure 1-12 below describes the outline of this study, in order to reach the Goals and Objectives:

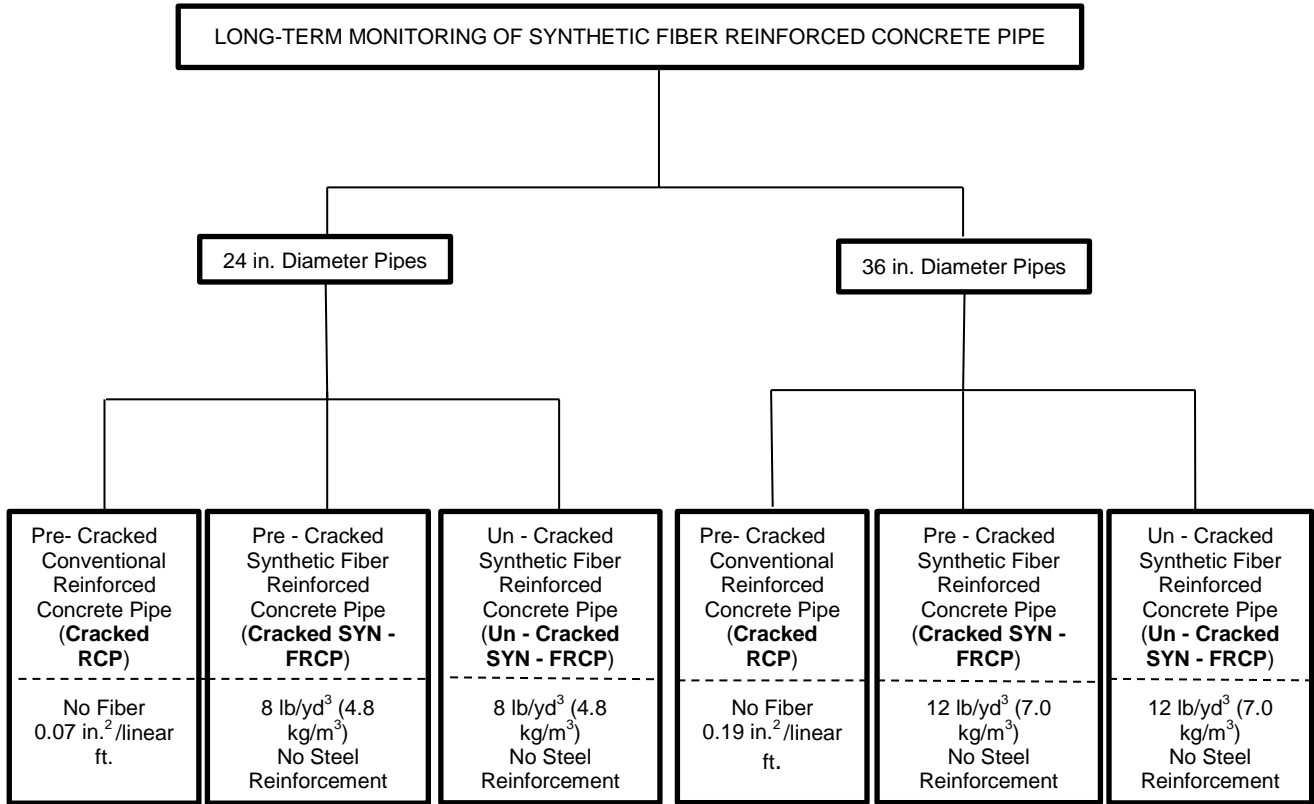


Figure 1-12 Outline of this Study

## Chapter 2

### Field Experimental Set-Up and Monitoring

#### 2.1 Location

The field test and monitoring were done at Hanson Pipe & Precast, Inc. 1000 MacArthur Blvd, Grand Prairie, TX, located along MacArthur Boulevard and Tom Landry Freeway (I-30). This is also where the pipe specimens were all produced. Figure 2-1 below shows the exact location at the plant for the field experimental set-up and monitoring.

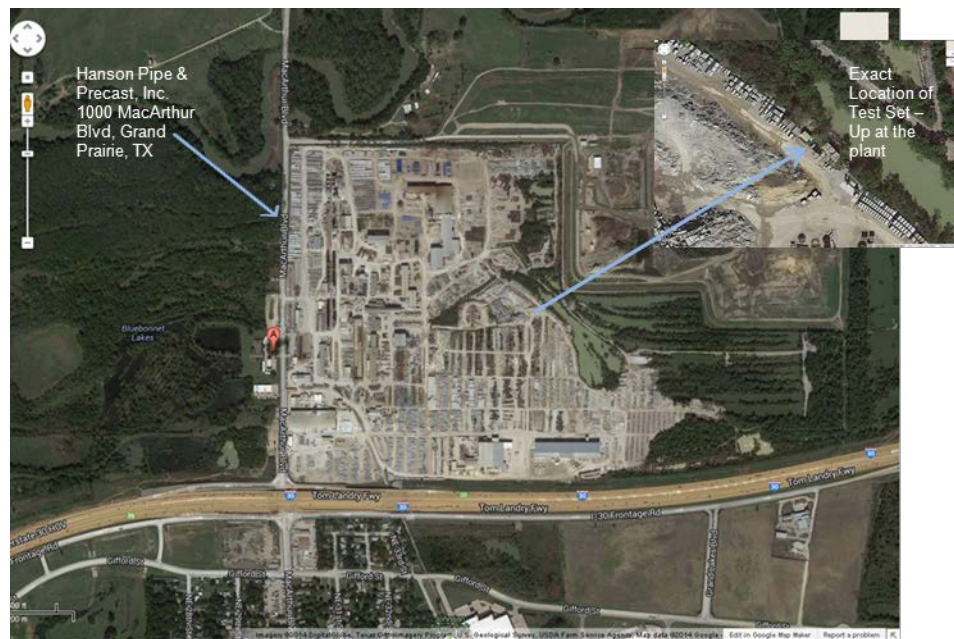


Figure 2-1 Location of test set-up and monitoring

## 2.2 Material Property

### Synthetic Fiber:

Synthetic fiber was used in this study, which was made from 100% virgin polypropylene. The fiber was a mono-filament and an embossed fiber (MasterFiber MAC Matrix) produced by BASF Corporations, in accordance to ASTM C1116. The fiber length was 2 in. (54mm) and the tensile strength was about 85kisi (585MPa). Previous applications of the MasterFiber MAC Matrix included slab-on-grade and shotcrete as a replacement for welded wire reinforcement. Table 2-1 below shows a brief mechanical and geometric property of the fiber used in this study

Table 2-1 Mechanical and Geometric Properties

Configuration	Surface Type	Materials	Length	Tensile Strength	Equivalent Diameter
Stick Type	Embossed	100% Virgin Polypropylene	2.0 in. (54 mm)	85 ksi (585 Mpa)	0.04 in. (0.9 mm)



Figure 2-2 MasterFiber MAC Matrix

#### Concrete Mixture:

As mentioned earlier, there are two types of methods of producing pre-cast concrete pipes, namely; wet cast and dry cast. For this study, dry- cast concrete was used which is also commonly referred to as zero-slump mix. The mix formulation of concrete used to acquire 28 day strength of 4000 psi (28 MPa) for class III, Wall B in accordance to ASTM C76, was as follows:

- 380 lb/yd<sup>3</sup> (226 kg/m<sup>3</sup>) of Type I/II Portland Cement.
- 125 lb/yd<sup>3</sup> (74 kg/m<sup>3</sup>) of Fly Ash.
- 1670 lb/yd<sup>3</sup> (990 kg/m<sup>3</sup>) of Aggregate.
- 1700 lb/yd<sup>3</sup> (1010 kg/m<sup>3</sup>) of Sand.
- 217 lb/yd<sup>3</sup> (129 kg/m<sup>3</sup>) of Water.

As a result, the water-cement ratio was 0.43. All the materials were dry mixed together for 2 minutes, together with the synthetic fibers. Water was then added to the mixture, and an additional 3 minutes of mixing was continued to ensure a thorough dispersion of the fibers after the addition of water. Type I/II cement were used in the mixture, to resist sulfate from the soil. Therefore, this mixture of the cement would help with corrosion of the buried underground pipes.

The Figure 2-3 below shows the typical synthetic fiber distribution in the dry mixture (zero-slump concrete):





Figure 2-3 Typical synthetic fiber distribution

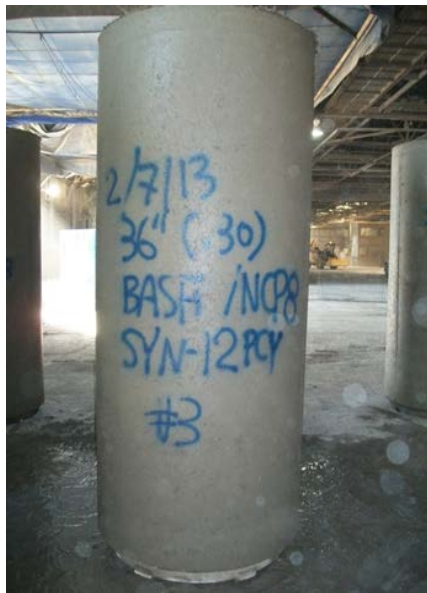
Test Specimen:

Two different sets of 8 ft. (2400 mm) long pipes with inside diameters of 24 in. (600 mm) and 36 in. (900 mm) were used. For the synthetic pipes, twelve pipes in total were produced for Class III strength using a Wall B, in accordance to ASTM C76 without a steel cage (steel reinforcement). On the other hand, as a control specimen, four regular reinforced concrete pipes were produced for Class III, Wall B were manufactured with steel reinforcement of 0.07 in<sup>2</sup>/linear ft. (150 mm<sup>2</sup>/linear m) and 0.19 in<sup>2</sup>/linear ft. (580 mm<sup>2</sup>/linear m) for the 24 in. and 36 in. regular reinforced concrete pipes, respectively. All the concrete pipes were casted the same day to reduce variability in the mechanical properties of the pipes, with the aging of concrete.

It is noted that, in order to simulate damaged pipes due to service loading, the pipe specimens were initially pre-cracked. In order to do this, the specimens were loaded until the first visible crack was observed on the crown and invert of the pipe, by using the three-edge-bearing test. As soon as the pre-cracks were observed and located on the

crown and invert, the loads were removed and the pipes were buried in the trenches, which will be further discussed in the next sections to follow.

The Figure 2-4 below shows the specimens produced of the 24 in. and 36 in. concrete pipes:



(a)



(b)

Figure 2-4 Pipe specimens produced; (a) Class III – 36 in. SYN-Pipe (12 lbs/yr3), (b) Class III – 24 in. SYN-Pipe (8 lbs/yr3)

### 2.3 Short-Term Test – Three-edge Bearing Test

As mentioned, in order to simulate damaged pipes, due to service loading, the specimens were cracked until the first initial cracks were seen on the crown and invert. For this crack to be achieved, the three-edge bearing test was performed.

The three-edge-bearing test (D-load test) was performed in accordance with ASTM C497 “Standard Test Method for Concrete Pipe, Manhole Sections, or Tile”. This standard basically is a description of a test whereby a machine is able to apply force along the length of the specimen being tested in order create a 0.01 in. crack or to achieve an ultimate load. Also, under this standard, the machine capable of applying such force must not yield at any part during the testing, be rigid in shape, and evenly distribute the load being applied.

This test requires that the specimen should be supported by one upper bearing strip and two parallel lower bearing strips. The upper bearing strip consists of a wood beam that’s attached to a steel beam which does deflect under pressure. The two lower bearing strips can be either be made from wood or rubber (in this study, rubber was used), which is fixed to a rigid base that is usually made of a wooden beam.

From the three-edge bearing test, the load-carrying capacity of the pipe, the sustained load level corresponding to the visual initial crack, and the suitable fiber dosage for the time-dependent experiment were determined. The D-Load value from the load-deflection graph is obtained from the following equation:

$$D_{ULT} = \frac{\text{Experimental load (lb)}}{\text{Diameter of pipe (ft)} \times \text{Length of Pipe (ft)}} \quad (9)$$

As shown in Figure 2-5, the rubber Bearing strips are placed at a distance apart of not more than 1 in./ft. of specimen diameter, but under no case, less than 1 in, in accordance to ASTM C497. Hence, for this study, the two sets of specimens, 24 in. and 36 in. diameter pipes would have a spacing of 2 in. and 3 in., respectively.

The testing schematic can be seen in the Figure 2-5 below:

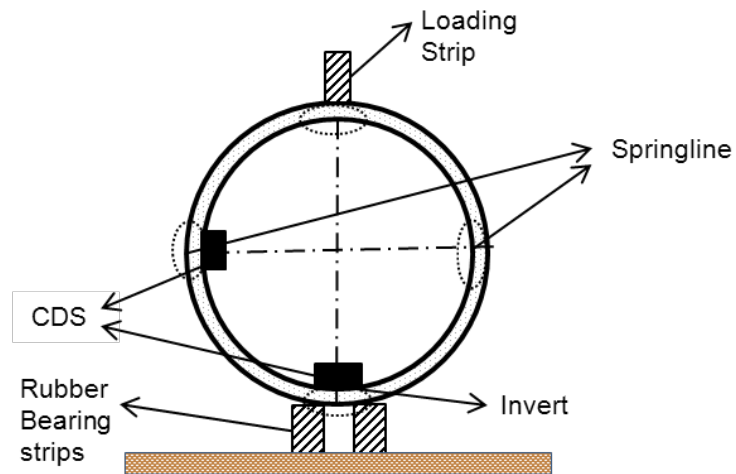


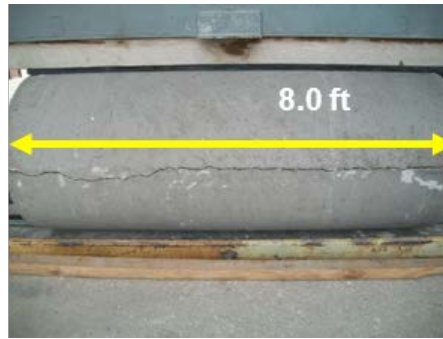
Figure 2-5 Schematic of three-edge bearing test

The apparatus used to do the test was a cable displacement sensor (CDS), which is basically a box with a cable that measures displacement. The CDS is connected to a computer and DAQ which record the data. The Figure 2-6 below shows the CDS being mounted to the pipe and ready for testing on the three-edge bearing test:



Figure 2-6 Cable displacement sensor

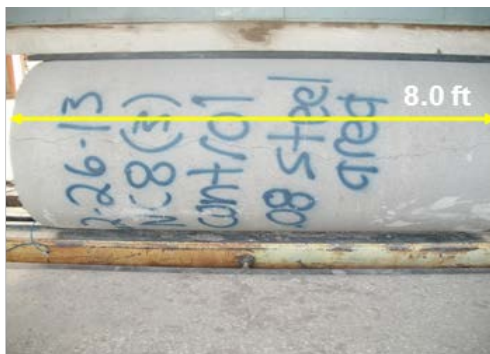
For the 24 in. Pipe specimens, the test-setup and crack pattern from the D-load is shown in following Figure 2-7 below:



(a)



(b)



(c)

Figure 2-7 Pipe test set up and crack pattern 24 in.; (a) Synthetic Fiber reinforced Pipe 6 PCY w/o steel cage, (b) Synthetic Fiber reinforced 8 PCY w/o steel cage, (c) Regular Reinforced Pipe

The main crack for both the regular reinforced concrete pipe and synthetic fiber pipe were observed to be at the invert of the pipe as shown below:



Figure 2-8 Main-crack at invert of 24. in pipes; (a) regular reinforced, (b) synthetic fiber reinforced

For the 36 in. Pipe specimens, the test-setup and crack pattern from the D-load is shown in following Figure 2-9 below:

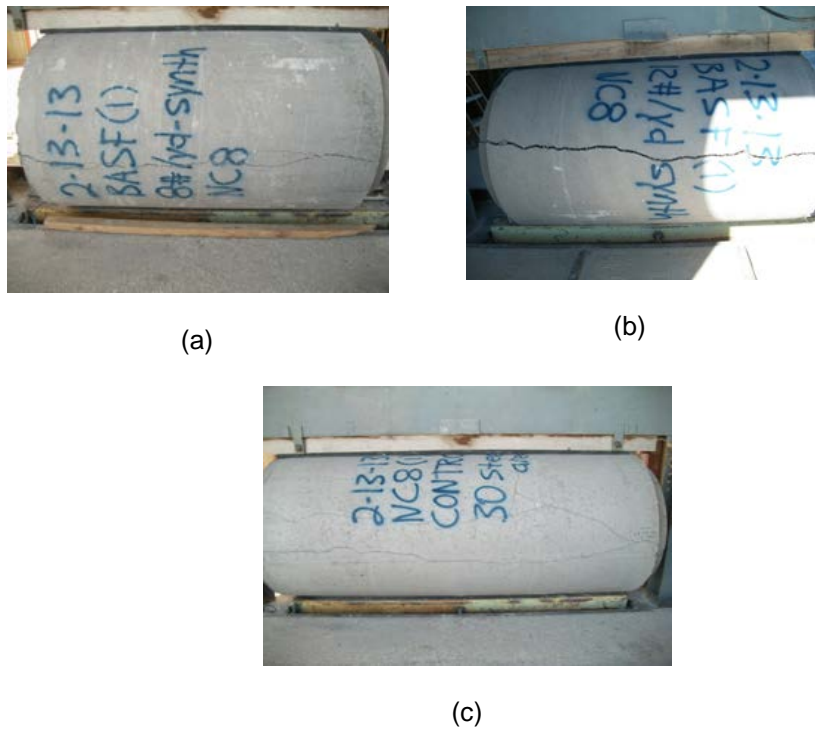


Figure 2-9 Pipe test set up and crack pattern 36 in.; (a) synthetic fiber reinforced pipe 8 PCY w/o steel cage, (b) synthetic fiber reinforced 12 PCY w/o steel cage, (c) regular reinforced pipe

The main cracks in the regular reinforced concrete pipes were at the crown, and on four sections of the synthetic fiber-reinforced concrete pipes; namely; Crown, Invert and the Spring-lines. The Figure 2-10 below shows the observation:



Figure 2-10 Cracks of 36 in. pipes; (a) regular reinforced pipe, (b) synthetic fiber reinforced pipe.

The D-Load vs. Vertical Deflection graph for the pipes are shown and discussed in section 2.4, under Test Results and Discussion

## 2.4 Long-Term Test – Buried Pipes

### 2.4.1 Detailed Construction

This experimental investigation included measurement of instantaneous and time-deformation behavior. In order to carry out the long-term performance of the buried regular reinforced pipes and synthetic fiber reinforced pipes, a number of steps were taken as follows:



Trenches:

Initially, two parallel trenches were excavated by using an excavator machine. Due to water collection from the ground, a narrow trench was excavated to by-pass the water collected in the trench into a nearby river, West Fork Trinity River. The pipes were placed with a steel capping. However due to the trench walls failing and collapsing, new trenches were excavated. Figure 2-11 below shows this:



(a)



(b)



(c)



(d)



(e)

Figure 2-11 Initial trench and failure; (a) Initial trench for 24 in. and 36 in.,(b) water collected in trench, (c) trench wall collapse, (d) different view of trench wall collapse, (e) trench excavated for de-watering of water collected



As a result of the trench walls falling, new trenches side by side were excavated, as shown in Figure 2-12 below:



(a)



(b)

Figure 2-12 New trenches excavated; (a) 24 in. pipe - trench, (b) 36 in. pipe trench

#### Instrumentation Headquarter:

An instrumentation headquarter was built to keep the DAQ system and for monitoring the experiment. The cables from the CDS box and the pressure sensors were connected to the computer to record the data. Once the data was recorded, it could be remotely accessed from the servers. Figure 2-13 below shows the instrumentation headquarters built for long-term monitoring:



(a)



(b)

Figure 2-13 Instrumentation headquarters; (a) computer & DAQ system, (b) outside view

Bedding:

A rough compaction was initially done to compact the trench. This was performed by using a box culvert attached to hook, by a chain that was tied to a forklift. The forklift raised and lowered its forks, so as to simulate a stomping action, and hence, compacted the ground. Next, further more compaction was done by using a jumping jack for more precise compaction. After the trench ground was compacted, a type 2 installation was carried out with a bedding thickness of 6 in. (150 mm) and standard proctor compaction of 95%. Table 2-2 shows the standard installation for a type 2 installation from the American Concrete Pipe Association's design manual.

Table 2-2 Standard installation and minimum compaction requirements from ACPA

Installation Type	Bedding Thickness	Haunch and Outer Bedding	Lower side
Type 2	$D_o/24$ minimum, not less than 3 in. (75 mm), If rock foundation, use $D_o/12$ minimum, not less than 6 in. (150 mm)	90% Category I or 95% Category II	85% Category I, 90% Category II, or 95% Category III

The bedding consisted of sand being dumped in the trench with a loader. The sand poured was spread out evenly by workers using a shovel. The bedding was then compacted with a jumping jack until the ground was firm. The ground was checked to make sure it was level, and prepared for the next stage; pipe placing. A plank of wood measuring the length of the pipe specimens, 8 ft. (2400 mm), was placed on the ground to mark on the trench for exact locations of the three pipes being placed in the trench ground. Figure 2-14 below shows the bedding process:



(a)



(b)



(c)

Figure 2-14 Bedding preparation-step 1; (a) Rough compaction,(b) compaction using jumping jack, (c) Soil added by loader for bedding

After the soil is added for bedding, the following Figure 2-15 below shows in detail the next process carried out to make the trench ready for pipe placement:



(a)



(b)



(c)



(d)



(e)

Figure 2-15 Bedding preparation-step 2; (a) spreading of soil, (b) compacting using jumping jack, (c) 6-7 in. bedding, (d) wooden plank for level and marking, (e) Markings on bedding for pipe placement

#### Pipe Placing and Steel Capping:

The pipe specimens were placed on the marked bedding with the help of a forklift that was attached to the pipe, via a chain, and guided by two persons in the trench for accurate placement. The forklift was then used to place steel capping on top of the pipes. The steel capping was laid-out around each pipe to enable access to the inside of the pipe, for later purposes during the test. The capping was designed not to make direct contact with the pipe, because the sharp steel edges of the cap would cause pressure on the pipe, hence cause cracking, which would interfere with the results of the experiment. Therefore, rubber strips were placed at the ends (connections) where the steel caps would sit. The capping with the lateral bracing was also used to keep the native soil or fine gravel, and backfill from flowing out.

It was noted that after the pipes were placed, and the steel capping was installed on the pipe (with the rubber strip), the cable displacement sensor (CDS) and the pressure inducer were installed before the back filling was done. This will be further discussed in the next section, 2.4.2 Instrumentation.

Pipe placing and steel capping is shown in Figure 2-16:





(a)



(b)



(c)



(d)



(e)



(f)

Figure 2-16 Pipe placing and steel capping; (a) forklift used for placing, (b) side view of three pipes placed, (c) placing of steel cap, (d) rubber strip placed at connections, (e) view of steel capping installed on rubber strips, (f) view of complete

Backfill up to Ground Level-step 1:

Here, the pipe with the steel capping was backfilled with the native soil. The soil was dumped with a loader and filled to the top of the pipe. During the backfilling process, the sand was compacted several times as the soil was poured in layers. The equipment used for compaction was the jumping jack. Figure 2-17 below shows the above described procedure



(a)



(b)



(c)



(d)

Figure 2-17 Backfill up to ground level-step 1; (a) backfill by native soil, (b) compaction (0.5D), (c) compaction (0.5D), (d) backfill to ground Level

Backfill up to Ground Level-step 2:

The native soil was poured into the trench, until the set-up was level with the ground. Once more, compaction was done by the jumping jack. The compaction ensured that the trench was firm and strong enough for the next step, placing of the box culverts. Trench wall bracings were added to the side that was not supported by the steel capping (i.e. the gap between the pipes installed). Figure 2-18 below shows this process in detail:



(a)



(b)



(c)



(d)

Figure 2-18 Backfill up to ground level-step 2; (a) compaction to ground level, (b) direction of buried pipes (24 in. pipes after backfill), (c) bracing between steel capping and trench wall bracing, (d) 36 in. pipes after backfill.



Surcharge by Concrete Culverts-step 1:

The final part of the construction was placing the concrete box culvert, which acted as the surcharge, and filling it with fine gravel. Once the compaction and backfill up to the ground was done, a forklift was used to place the box culvert exactly on the steel capping. Dimensions of the first box culvert are as follows:

**Width = 10 ft (3000 mm)**

**Height = 8 ft (2400 mm)**

**Length = 8 ft (2400 mm)**

Once the box culvert was placed on the steel capping, a loader filled it up with fine gravel. It was noted that the box culvert did not have a slab, due to the gravel acting as the overburden load; hence, no need of a bottom slab. Figure 2-19 below shows the set-up of the first culvert:



(a)



(b)



(c)



(d)

Figure 2-19 Placing of concrete culvert-step 1; (a) Placing of concrete culvert, (b) Dimension of culvert, (c) Height of culvert, (d) Placing of culvert

Surcharge by Concrete Culverts-step 2:

Once the first box concrete culvert was placed, another box culvert was staked on the first one, and the same process was repeated in filling the culvert up with fine gravel, as done previously. A forklift is used to place the culvert onto the previous one, and the loader fills it up till the top with fine gravel. Once more, this culvert did not have a slab bottom like the first culvert; to allow the gravel poured to act as the sustained load on the pipe below it. The total height of the two culverts in both the trenches was 14ft. (4200 mm). Dimensions of the second box culvert are as follows:

**Width = 10 ft (3000 mm)**

**Height = 6 ft (1800 mm)**

**Length = 8 ft (2400mm)**

The Figure 2-20 shows the set-up of the second culvert:



(a)



(b)



(c)



(d)

Figure 2-20 Placing of concrete culvert-Step 2; (a) Loader dumping of Pea gravel, (b) culvert filled with gravel, (c) stacking of culverts, (d) total height of culverts, 14 ft. (4200 mm)

It is noted that the experimental set-ups for both the 24 in. pipe and 36 in. pipe were exactly the same. However, one difference in the set-up was the trench width excavated; 7ft. (2000 mm) and 8 ft. (2400 mm) for the 24 in. pipe and 36 in. pipe, respectively. This difference of 1 ft. (300 mm) was due to the 36 in. diameter pipe being a feet bigger than the 24.in pipe. The second difference was, the height of the native soil above the concrete pipes, which was backfilled up to the ground level. To clarify, in order to simulate the long-term sustained load, a height of native soil of 2ft. (600 mm) and 4 ft. (1200 mm) were backfilled for a 24 in. and 36 in. pipe, respectively. The long-term sustained load simulated, is also discussed more in detail in section 2.4.3, Applied Load.

The final step-up of all the six pipes for the time-dependent behavior monitoring is shown in the figure below:



Figure 2-21 Final set-up for long-term monitoring

More detailed photographs of the 24 in. (600 mm) and 36 in. (900 mm) pipe set-ups can be found in Appendix A.

#### 2.4.2 Instrumentation

After the pipe placing, and steel capping of the pipe, the sensors were installed before backfilling was done. The sensors for this experiment were cable displacement sensors (CDS), to measure vertical deflection of the pipes, and pressure transducers, for vertical and lateral pressure. It is noted that, the cable displacement sensors were placed on the crown, so as not to be affected by rain and/or water collected at the invert, or to prevent damage by soil falling back into the pipe, due to the CDS being a very sensitive device. Figure 2-22 below shows the instruments used:



Figure 2-22 Sensors for long-term monitoring; (a) cable displacement sensor (CDS), (b) Pressure transducer (semi-conductor type)

The CDS was placed on the invert by using a glue gun. One end of the cable used to transfer data was connected to the outlet slot of the CDS, while the other end was connected to the DAQ system. The pressure transducer was mounted on a wooden plank, so as to act as a flat surface for accurate measurement of pressure being applied by the soil, as the surface of the pipe itself, is curved and not flat. The Figure 2-23 below shows the set-up of the two sensors:



(a)



(b)

Figure 2-23 Installation of sensors; (a) cable displacement sensors, (b) pressure transducers.



### 2.4.3 Applied Load

For the 24 in. pipe, a total overburden load of 16 ft. (4800 mm) and 18 ft. (5500 mm) for the 36 in. pipe was applied to simulate the sustained load. In accordance to ASTM C76, the sustained load level was determined as the service D-load ( $D_{0.01}$ ) of 1350 lb/ft/ft (65 kN/m/m), which corresponded to 68% and 81% of the peak D-load of the regular reinforced concrete pipes and the synthetic reinforced concrete pipes, respectively. In other words, the 2 ft. (600 mm) of silt backfilled above the pipe to the ground level, was calculated for the 24 in. pipe to provide the sustained load required to design a Class III, Wall B pipe by ASTM C76, and the 4 ft. (1200 mm) of silt clay was calculated to provide the sustained load for the 36 in. pipe in accordance to ASTM C76. It is noted that these heights calculated, in addition with the fixed 14 ft. (4200 mm) of pea gravel, provide the total overburden load needed to simulate the sustained load. Figure 2-24 below shows the schematic of the sustained load heights calculated.

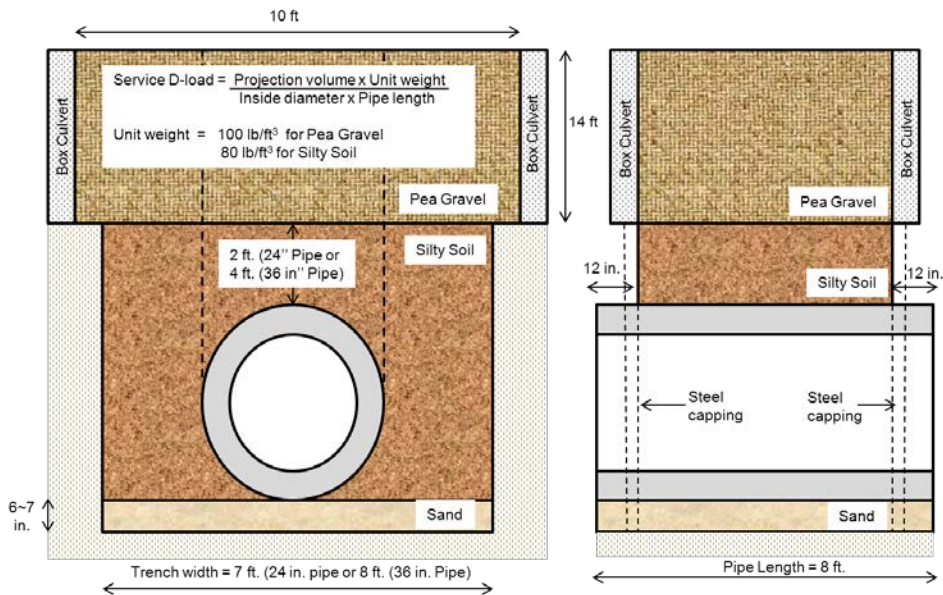


Figure 2-24 Schematic of overburden load



Calculation of the sustained load is as follows:

For the 24 in. (600 mm) pipe:

$$\text{Load} = (\text{Length}(\text{ft.}) \times \text{Height}(\text{ft.}) \times \text{Length}(\text{ft.})) \times \text{Unit Weight of Soil} \left(\frac{\text{lb}}{\text{ft}^3}\right)$$

Therefore, the total load from the pea gravel and silty soil is calculated as follows:

$$\text{Load} = ((2 \text{ ft.} \times 14 \text{ ft.} \times 5.5 \text{ ft.}) \times 100 \frac{\text{lb}}{\text{ft}^3}) + ((2 \text{ ft.} \times 2 \text{ ft.} \times 5.5 \text{ ft.}) \times 80 \frac{\text{lb}}{\text{ft}^3})$$

$$\text{Load} = (15400 \text{ lb}) + (1760 \text{ lb})$$

$$\text{Load} = 17160 \text{ lb}$$

From the D-load equation:

$$D - \text{load} = \frac{\text{Experimnetal load (lb)}}{\text{Diameter of pipe (ft.)} \times \text{Length of pipe (ft.)}}$$

$$D - \text{load} = \frac{17160 \text{ lb}}{2 \text{ ft.} \times 5.5 \text{ ft.}} = 1560 \text{ lb}$$

For the 36 in. (900 mm) pipe:

$$\text{Load} = (\text{Length}(\text{ft.}) \times \text{Height}(\text{ft.}) \times \text{Length}(\text{ft.})) \times \text{Unit Weight of Soil} \left(\frac{\text{lb}}{\text{ft}^3}\right)$$

Therefore, the total load from the pea gravel and silty soil is calculated as follows:

$$\text{Load} = ((3 \text{ ft.} \times 14 \text{ ft.} \times 5.5 \text{ ft.}) \times 100 \frac{\text{lb}}{\text{ft}^3}) + ((3 \text{ ft.} \times 4 \text{ ft.} \times 5.5 \text{ ft.}) \times 80 \frac{\text{lb}}{\text{ft}^3})$$

$$\text{Load} = (23100 \text{ lb}) + (5280 \text{ lb})$$

$$\text{Load} = 28380 \text{ lb}$$

From the D-load equation:

$$D - \text{load} = \frac{\text{Experimnetal load (lb)}}{\text{Diameter of pipe (ft.)} \times \text{Length of pipe (ft.)}}$$

$$D - \text{load} = \frac{28380 \text{ lb}}{3 \text{ ft.} \times 5.5 \text{ ft.}} = 1720 \text{ lb}$$

From the calculations shown above, the D-load was greater than required as per ASTM C76 specification for class III pipe (1350 lb/ft/ft). For the 24 in. (600 mm) diameter pipe, the calculated height of silt was obtained at 2 ft. (600 mm). For the 36 in. (900 mm) diameter pipe, the calculated height of silt was obtained at 4 ft. (1200 mm).

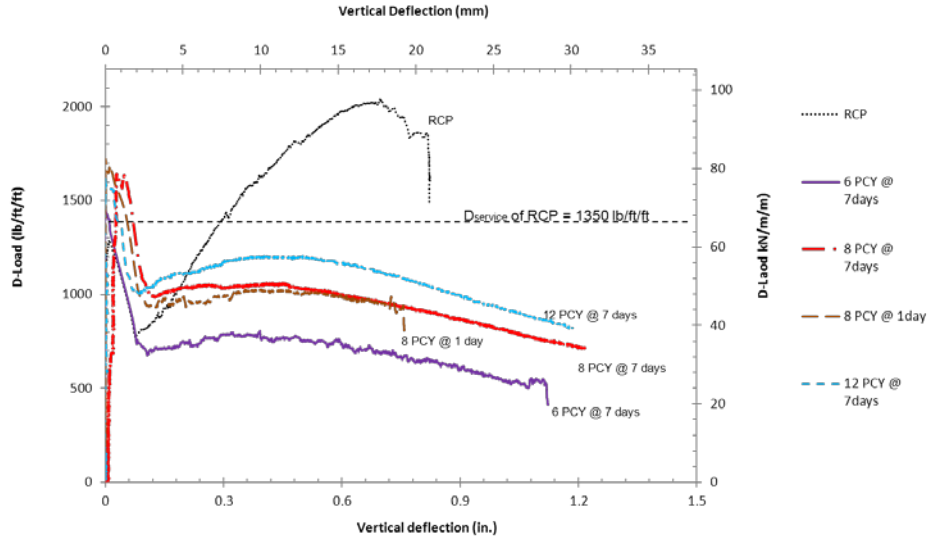
## 2.5 Test results and Discussion

### 2.5.1 Short-Term Response – Three-Edge Bearing Test

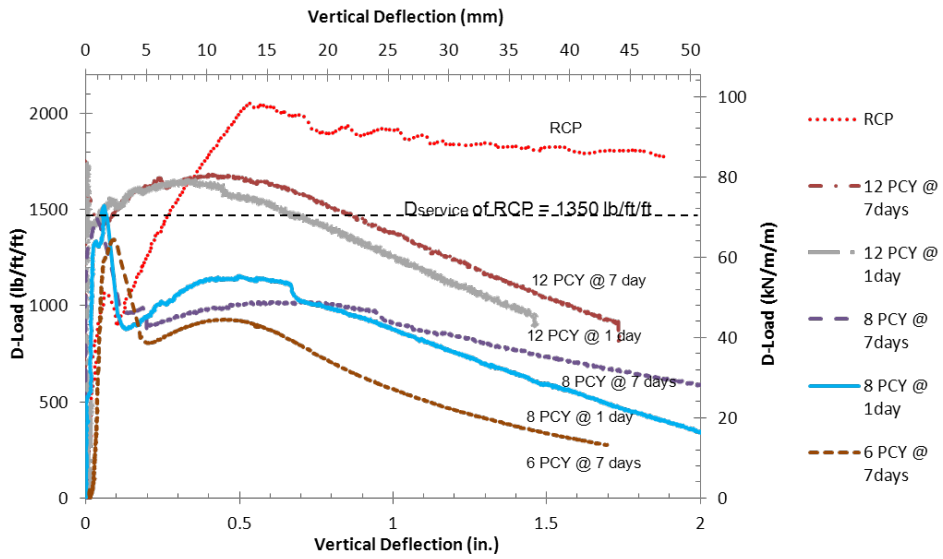
The values obtained from the Three-Edge bearing test, were used to plot the load-deflection curve for both the 24 in. and 36 in. pipe. It is noted that when 5% of change was observed in the vertical diameter, the testing was stopped.

For the 24 in. synthetic pipes, the maximum Peak D-Load were 1431 lb/ft/ft (68.5kN/m/m), 1695 (81.1 kN/m/m) and 1594 lb/ft/ft (76.3 kN/m/m), for 6 lb/yd<sup>3</sup> (3.5 kg/m<sup>3</sup>), 8 lb/yd<sup>3</sup> (4.8 kg/m<sup>3</sup>) and 12 lb/yd<sup>3</sup> (7.0 kg/m<sup>3</sup>) fiber dosages, respectively. An increase of 11.3% in D-load strength was observed for increase of fiber dosage from 6 lb/yd<sup>3</sup> (3.5 kg/m<sup>3</sup>) to 12 lb/yd<sup>3</sup> (7.0 kg/m<sup>3</sup>). From Figure 2-25 (a), the graph of D-load vs Vertical Deflection, it is observed that fiber dosage of 8 lb/yd<sup>3</sup> (4.8 kg/m<sup>3</sup>) is the best for providing Peak D-load strength, compared to the other fiber dosages used.

For the 36 in. Synthetic pipes, the maximum Peak D-load were 1313 lb/ft/ft (62.8 kN/m<sup>3</sup>), 1486 lb/ft/ft (71.1 kN/m/m) and 1738 lb/ft/ft (83.2 kN/m/m), for 6 lb/yd<sup>3</sup> (3.5 kg/m<sup>3</sup>), 8 lb/yd<sup>3</sup> (4.8 kN/m/m) and 12 lb/yd<sup>3</sup> (7.0 kg/m<sup>3</sup>) fiber dosages, respectively. An increase of 32.3% in D-load strength was observed for increase of fiber dosage from 6 lb/yd<sup>3</sup> (3.5 kg/m<sup>3</sup>) to 12 lb/yd<sup>3</sup> (7.0 kg/m<sup>3</sup>). From Figure 2-25 (b), the graph of D-load vs. Vertical Deflection, it is observed that fiber dosage of 12 lb/yd<sup>3</sup> (7.0 kg/m<sup>3</sup>) is the best for providing Peak D-load strength, compared to the other fiber dosages used.



(a)



(b)

Figure 2-25 Load-deflection curves from three-edge bearing test; (a) for 24 in. pipes, (b) for 36 in. pipes

Synthetic fiber reinforced concrete pipes, with greater fiber dosages, roughly provide a higher D-load in terms of Peak D-load. However, an increase of about half in fiber dosages from 8 lb/yd<sup>3</sup> (4.8 kg/m<sup>3</sup>) to 12 lb/yd<sup>3</sup> (7.0 kg/m<sup>3</sup>), did not show similar percentage increases in D-load Strength. It was observed that all the fiber dosages tested, showed the ability to resist brittle failure in plain concrete pipes, due to ductility and energy absorption capacity being improved. Hence, the pipe can undergo large deformations, without collapse. The most significant benefit of synthetic fiber reinforcement in concrete is flexural toughness, which represents the post-cracking behavior, as opposed to strength. The data obtained from the graphs was used to estimate the sustained load level, and the appropriate fiber dosages for the pipes. Observing the Peak D-load and the post cracking behavior, it is noted that fiber dosages of 8 lb/yd<sup>3</sup> (4.8 kg/m<sup>3</sup>) for the 24 in. (600 mm) pipe, and 12lb/yd<sup>3</sup> (7.0 kg/m<sup>3</sup>) for the 36 in. (900 mm) pipe were most appropriate for this experiment.

The data for the graph of D-load vs. Vertical Deflection for both, the 24 in. (600 mm) and 36 in. (900 mm) pipes, along with the most appropriate fiber dosages (highlighted in red) for both sizes of pipes of 24 in. (600 mm) and 36 in. (900mm) are summarized in the Table 2-3 below:

Table 2-3 Test result for Three-edge bearing test

Specification		Cracking D-load Corresponding the First Visual Crack ( $D_{cr}$ )		Peak D-load Capacity ( $D_{ult}$ )	
		lb/ft/ft (kN/m/m)	Increasing (%)	lb/ft/ft (kN/m/m)	Increasing (%)
24in. (600mm) Pipes	RCP: 0.07 in <sup>2</sup> /ft (148.2 mm <sup>2</sup> /m) @7-days	1285 (61.5)	-	2040 (97.7)	-
	SYN-FRCP: 6 lb/yd <sup>3</sup> (3.5 kg/m <sup>3</sup> ) @7-days	1372 (65.6)	7%	1431 (68.5)	-30%
	SYN-FRCP: 8 lb/yd <sup>3</sup> (4.8 kg/m <sup>3</sup> ) @1-day	1551 (74.2)	21%	1636 (78.3)	-20%
	SYN-FRCP: 8 lb/yd <sup>3</sup> (4.8 kg/m <sup>3</sup> ) @7-days	1539 (73.6)	20%	1695 (81.1)	-17%
	SYN-FRCP: 12 lb/yd <sup>3</sup> (7.0 kg/m <sup>3</sup> ) @7-days	1496 (71.6)	16%	1594 (76.3)	-22%
36 in. (900 mm) Pipes	RCP: 0.09 in <sup>2</sup> /ft (190.5 mm <sup>2</sup> /m) @7-days	1066 (51.1)	-	2050 (98.2)	-
	SYN-FRCP: 6 lb/yd <sup>3</sup> (3.5 kg/m <sup>3</sup> ) @7-days	1217 (58.2)	14%	1313 (62.8)	-36%
	SYN-FRCP: 8 lb/yd <sup>3</sup> (4.8 kg/m <sup>3</sup> ) @1-day	1305 (62.4)	22%	1477 (70.7)	-28%
	SYN-FRCP: 8 lb/yd <sup>3</sup> (4.8 kg/m <sup>3</sup> ) @7-days	1358 (65.0)	27%	1486 (71.1)	-28%
	SYN-FRCP: 12 lb/yd <sup>3</sup> (7.0 kg/m <sup>3</sup> ) @1-day	1592 (76.2)	49%	1664 (79.6)	-19%
	SYN-FRCP: 12 lb/yd <sup>3</sup> (7.0 kg/m <sup>3</sup> ) @7-days	1638 (78.4)	54%	1738 (83.2)	-15%

Regardless of the pipe size, it was observed that synthetic fiber reinforced pipes had one-line cracks patterns which were primarily located at the crown, invert and spring-lines. This was observed to be a 5% change in the vertical diameter of the pipe. Regular reinforced concrete pipes had circumferential cracks that were observed along the circumference of the cross section of the pipe. This is due to regular reinforced concrete pipe undergoing shear and deboning type cracks. Also, multiple crack patterns were seen on the outer surface of the regular reinforced concrete pipes. Figure 2-26 below shows this:



(a)



(b)

Figure 2-26 Crack pattern; (a) for synthetic fiber reinforced concrete pipe (b) for regular reinforced concrete pipe

### 2.5.2 Long-Term Response – Time-Dependent Behavior

The results of the tests, which were aimed at monitoring the incremental vertical deformation of cracked regular reinforced and un-cracked synthetic reinforced concrete pipes are shown in the Table 2-3 and graphs in Figure 2-27 and Figure 2-28. The measurement of the incremental vertical deflections, were recorded as soon as fine gravel was poured into the second box culvert, after being stacked on the first. It is noted that the recorded data fluctuated slightly due to environmental factors, such as rainfall falling going through the gravel in the box culvert, or wind blowing, which could affect the sensitive cable displacement sensor (CDS). Other factors that may have fluctuated the data recorded could be due to aggregates from the plant being thrown in the openings (for serviceability) between the pipe joints, while workers move aggregates around the plant for production purposes where needed. As soon as sustained loading was applied, the time-dependent deformation started immediately. It was observed that the time-dependent deformation increased with constant sustained loading with time. However, the change of the time-dependent deformation was not significant with time in all cases of the 24 in. and 36 in. concrete pipes. For up to 9000 hours, the maximum change of deformation was 3% for the cracked 24 in. (600 mm) synthetic fiber reinforced concrete pipe with the fiber dosage of 8 lb/yd<sup>3</sup> (4.8 kg/m<sup>3</sup>); whereas, the maximum change of deformation was 2.3% for the cracked 36 in. (900 mm) synthetic fiber reinforced concrete pipe with fiber dosage of 12 lb/yd<sup>3</sup> (7.0 kg/m<sup>3</sup>). It was noted initially, in the pipe set-up and installation, that un-cracked 24 in. (600 mm) and 36 in. (900 mm) synthetic reinforced concrete pipes, were considered. However, in data collection for the time-dependent deformation graphs, they were omitted because as soon as the sustained loads were applied, the un-cracked pipes for both diameter sizes cracked. Hence, the un-cracked

pipe behaved as a cracked pipe, and the result would be identical with that of the initial pre-cracked pipe. Therefore, the study only compared the time-dependent deformation for the cracked synthetic and cracked regular reinforced pipes for both diameter sizes.

Table 2-4 Summary of measured vertical deformation up to 9000 Hours

Specification		Instantaneous Deflection		Time-Dependent Deflection		Total Deflection
		in. (mm)	% of total deflection	in. (mm)	% of total deflection	in. (mm)
24 in. (600mm) Pipes	Cracked RCP: Control	0.10 (2.54)	25	0.30 (7.62)	75	0.40 (10.16)
	Cracked SYN-FRCP: 8 lb/yd <sup>3</sup> (4.8 kg/m <sup>3</sup> )	0.19 (4.83)	18	0.86 (21.84)	82	1.05 (26.70)
36 in. (900 mm) Pipes	Cracked RCP: Control	0.08 (2.03)	13	0.52 (13.21)	87	0.60 (15.24)
	Cracked SYN-FRCP: 12 lb/yd <sup>3</sup> (7.0 kg/m <sup>3</sup> )	0.18 (4.57)	22	0.64 (16.26)	78	0.82 (20.83)

After 2000 hours, the time-dependent deformations for all pipes seemed to have stabilized, regardless of the size of pipe. However, at 1600 hours, rapid increase in deflection was observed in the 24 in. (600 mm) pre-cracked synthetic fiber reinforced concrete pipe. The reason for this behavior is due to development of localized cracks. It is noted that the time-dependent deformations were mostly reliant on the fiber dosage, and cracked pipes showed a larger total deformation (for same diameter pipes), regardless of the pipe size. In other words, higher fiber dosage pipes of 12 lb/yd<sup>3</sup> ( 7.0 kg/m<sup>3</sup>), slowed fiber pull out at the localized cracks better compared to the lower fiber dosage pipes of 8 lb/yd<sup>3</sup> (4.8 kg/m<sup>3</sup>).



From the summary of Table 2-3 above, it is observed that the total deformation of 24 in. (600 mm) pipes was 0.40 in. (10.66 mm), and 1.05 in. (26.70 mm), for the cracked regular reinforced pipe, and cracked synthetic reinforced pipe, respectively. Whilst the instantaneous deformations were 0.10 in. (2.54 mm), and 0.19 in. (4.83 mm). The time-dependent deformations were 0.33 in. (7.62 mm), and 0.86 in. (21.84 mm). Lastly, the percent changes in deformation were 1.5%, and 3.0% for the cracked regular reinforced pipe and cracked synthetic reinforced pipe, respectively.

Observing the summary of Table 2-3 above, for the 36 in. (900 mm) pipes, the total deformation was 0.60 in. (15.24 mm), and 0.82 in. (20.83 mm) for the cracked regular reinforced pipe, and cracked synthetic reinforced pipe, respectively. The instantaneous deformations were 0.08 in. (2.03 mm) and 0.18 in. (4.57 mm). The time-dependent deformations were 0.52 in. (13.21 mm), and 0.64 in. (16.26 mm). Lastly, the percent changes in deformation were 1.5%, and 2.2% for the cracked regular reinforced pipe and cracked synthetic reinforced pipe, respectively.

Figure 2-27 and Figure 2-28 show the graphs for the time-dependent behaviors, for the 24 in. (600 mm) and 36 in. (900 mm) pipes, respectively:

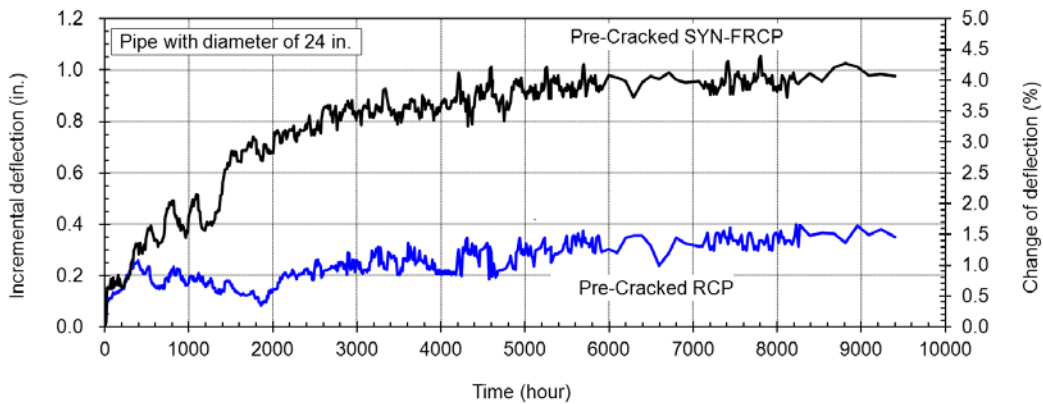


Figure 2-27 Time-dependent behavior for 24 in. (600 mm) pipes

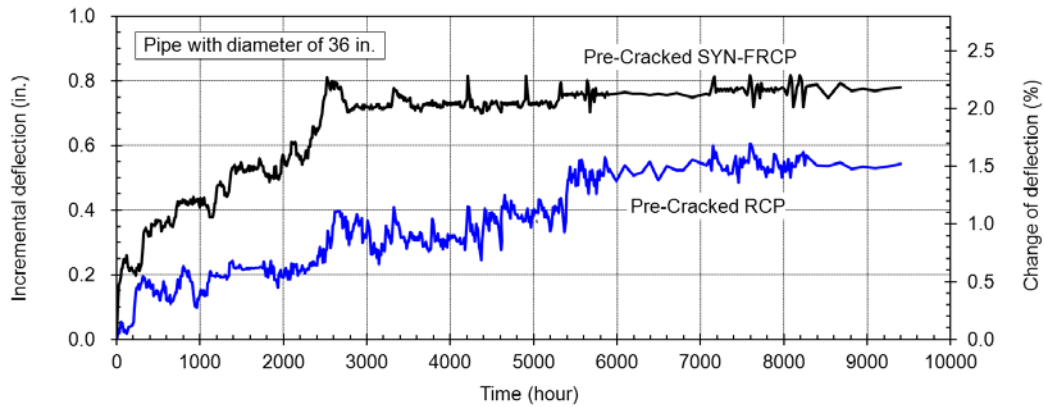


Figure 2-28 Time-dependent behavior for 36 in. (900 mm) pipes

It was found that no significant differences of change ( $\sim 0.8$  in. for the 24 in. pipe and  $\sim 0.4\%$  for the 36 in. pipe) in vertical diameter of the regular and synthetic reinforced concrete pipes were observed. Furthermore, it can be concluded that the difference between the change of deflection of 3.0%, for the cracked synthetic fiber reinforced concrete, and 1.5% for the cracked regular reinforced concrete, for the 24 in. (600 mm) pipe, was not significant. This is due to the sustained load of the synthetic and regular reinforced concrete pipe, being applied at 81% and 68% of the Peak D-load, respectively. A given criterion for synthetic and regular reinforced concrete pipe will be similar to the one for synthetic fiber reinforced concrete pipe which is currently being balloted. As a result, a factor of safety away from the specified ultimate load will be designed for synthetic fiber reinforced concrete pipes. Pre-cracked synthetic fiber reinforced concrete pipes, were included in this study to assess pipe performance under extreme and rare conditions (e.g. over-load or poor production. The long-term deformation of the pre-cracked synthetic fiber reinforced concrete pipe under the mentioned above condition, did not exceed 3%, which was not significant.

### 2.5.3 Crack Width

Figure 2-29 below shows the development of crack width in the synthetic fiber reinforced concrete pipe, after 600 hours, 1200 hours and 4000 hours, respectively, for the 24 in. (600 mm) pipe. For the pre-cracked pipes to be tested, it was important to crack the pipes before testing, ensuring not to cause large cracks. From the Three-edge bearing test, the pre-cracks on the crown were 0.006 in. (0.15 mm) and 0.008 in. (0.21 mm) on the invert, for the 24 in. (600 mm) synthetic fiber reinforced concrete pipe. It is noted that the pre-crack widths did not exceed the service state crack width of 0.01 in. (0.25 mm). However, after 600 hours, the same cracked pipe section increased in crack by 0.01 in. (25 mm), and 0.04 in. (1.02 mm) in the crown and invert, respectively. After 1200 hours, the same cracked pipe section increased in crack by 0.05 in. (1.27 mm), and 0.09 in. (2.28 mm) in the crown and invert, respectively. After a total of 4000 hours, the same cracked pipe section increased in crack by 0.07 in. (1.78 mm), and 0.1 in. (2.54 mm) in the crown and invert, respectively. It was observed that after 4000 hours, and until the 9000 hours of monitoring carried out for this study, the crack width in the same section continued to increase, but at very small increments, that were very insignificant.

The Figure 2-29 below shows the crack width developed over the monitoring:

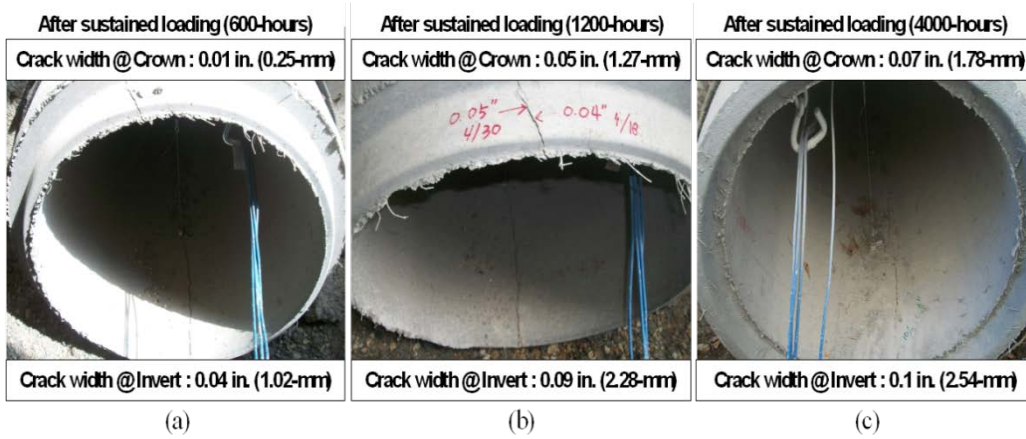


Figure 2-29 Crack propagation of the 24 in. cracked SYN-FRCP; (a) 600 hours after sustained loading, (b) 1200 hours after sustained loading, (c) 4000 hours after sustained loading

## Chapter 3

### Summary and Conclusion

It is important to compare time-dependent performance of synthetic fiber reinforced concrete to regular reinforced concrete, as synthetic fiber reinforced concrete is a new concept being introduced in the USA. In this study, both the short term and long term studies for regular reinforced and synthetic fiber reinforced concrete pipes were performed. Test results obtained from the three-edge bearing test have been used to verify that synthetic fibers are an effective way of improving mechanical properties of concrete pipes in dry-cast manufacturing. As for the time-dependent deformation, it was observed that the increased deformation in synthetic fiber reinforced concrete was not significant; a difference of 2.5% and 0.7% with regular reinforced and synthetic reinforced concrete pipe, respectively. Other observations made from this study include:

- From the load-deformation graphs, a higher fiber dosage of synthetic fiber reinforced concrete pipes provide, to some extent a higher Peak D-Load. But, with an increase of half the fiber dosage from 8 lb/yd<sup>3</sup> (4.8 kg/m<sup>3</sup>) to 12 lb/yd<sup>3</sup> (7.0 kg/m<sup>3</sup>), the same percentage increase in D-load strength was not observed.
- The three-edge bearing test showed that regardless of the size of the pipe specimen, flexural cracks were observed along the crown, invert and spring-lines for synthetic fiber reinforced concrete pipes. Also, shear cracks were not observed at the most critical deformation enforced during the testing.
- From the long-term monitoring of buried pipes, it can be concluded that the change in vertical deformation of the 24 in. (600 mm) pipes was, 1.5%, and 3.0% for the cracked regular reinforced pipe, and cracked synthetic reinforced pipe, respectively. The change in vertical deformation of the 36 in. (900 mm) pipes

were, 1.5%, and 2.2% for the cracked regular reinforced pipe, and cracked synthetic reinforced pipe, respectively.

- It can be concluded that, under severe and rare conditions, such as over-load or poor production, the maximum percent change in deformation did not exceed 3%, which is also insignificant, for pre-cracked synthetic fiber reinforced concrete pipes. Typically, this is not a condition which pipes undergo at service load. However, in order to study the crack resistance capability (pull-out) in comparison with time, pre-cracked pipes were included in this experiment.
- The specimens were designed for a class III reinforced concrete pipe. However, from the results observed in the three-edge bearing test, the specimens behaved more like a class II pipe. Therefore, there was an overload in the sustained load calculated.

Basically, regardless of the pipe sizes buried, the load-carrying capacity of the pipes increased with the addition of BASF fiber dosages added. Furthermore, synthetic fiber-reinforced concrete pipes performed well in keeping together the pre-cracked pipe, and preventing collapse by not exceeding 3% of change of the inside diameter during the 9000 hours of testing.

Appendix A

Pipe Set-Up

24 in. (600 mm) and 36 in. (900 mm)



Figure A-1 Photograph of trench excavated





Figure A-2 Photograph of Trench excavated for drainage system



Figure A-3 Photograph of drainage installation



Figure A-4 Photograph of rough compaction of initial trench





Figure A-5 Photograph of initial compaction of trench



Figure A-6 Photograph of pouring of sand for bedding



Figure A-7 Photograph of compaction of bedding





Figure A-8 Photograph of leveling check for bedding



Figure A-9 Photograph of bedding marked for pipe placement





Figure A-10 Photograph of pipe being placed



Figure A-11 Photograph of all three pipes placed in trench



Figure A-12 Photograph for placing of steel capping-step 1





Figure A-13 Photograph for placing of steel capping-step 2



Figure A-14 Photograph of rubber strips placed



Figure A-15 Photograph of rubber strip and steel capping installed





Figure A-16 Photograph of final set-up of steel capping for three pipes



Figure A-17 Photograph of CDS device installed at crown





Figure A-18 Photograph of pressure transducer installed

## References

1. Abolmaali, A., Mikhaylova A., Wilson, A., and Lundy, J. *Performance of Steel Fiber Reinforced Concrete Pipes*. Transportation Research Board Journal, 2012
2. Alhozaimy, A. M., Soroushian, P., and Mirza, F. Mechanical Properties of Polypropylene Fiber Reinforced Concrete and the Effects of Pozzalanic Materials. *Cement and Concrete Composites*, Vol. 18, 1996, pp.85-92.
3. ASCE 15-98 Standard Practice for Direct Design of Buried Precast Concrete Pipe Using Standard Installations (SIDD). *American Society of Civil Engineers*, 1998.
4. ASTM C1116 Standard Specification for Fiber-Reinforced Concrete. *American Society for Testing and Materials*, 2011.
5. ASTM C497 Standard Test Method for Concrete Pipe, Manhole Sections, or Tile. *American Society for Testing and Materials*, 2005.
6. ASTM C76 Standard Specification for Reinforced Concrete Culvert, Storm Drain and Sewer Pipe. *American Society for Testing and Materials*, 2011.
7. ASTM C76M Standard Specification for Reinforced Concrete Culvert, Storm Drain, and Sewer Pipe (Metric). *American Society for Testing and Materials*, 2011.
8. Atis, C.D., Karahan, O., K. Ari, Sola, O.C., and Bilim, C. Relation between Strength Properties (Flexural and Compressive) and Abrasion Resistance of Fiber (Steel and Polypropylene)-Reinforced Fly Ash Concrete. *Journal of Materials in Civil Engineering*, Aug.2009, Vol. 21, Issue 8, pp. 402-408. DOI:10.1061/(ASCE)0899-1561(2009)21:8(402).
9. BASF Corp. MasterFiber MAC Matrix. *Concrete Construction*. N.p., n.d. Web. 6 Apr. 2014. <<http://www.concreteconstruction.net/products/basf-corp.aspx>>.

10. Concrete Pipe Design Manual. *American Concrete Pipe Association*, 2007.
11. Concrete Pipe Handbook. *American Concrete Pipe Association*, 1998.
12. Concrete Pipe Technology Handbook. *American Concrete Pipe Association*, 1993.
13. Cunha, V.M., Barros, J.A., and Sena-Cruz, J. Pullout Behavior of Steel Fibers in Self-Compacting Concrete. *Journal of Materials in Civil Engineering*, Jan. 2010, Vol. 22, Issue 1, pp. 1-9. DOI: 10.1061/ (ASCE) MT.1943-5533.0000001.
14. Henry R. An Investigation of Large Diameter Fiber Reinforced Concrete Pipe. *ACI Special Publications*, Vol. 44, Np. SP44-25, 1974, pp. 435-454.
15. Kurtz, S., and Balaguru, P. Postcrack Creep of Polymetric Fiber-reinforced Concrete in Flexure. *Cement and Concrete Research*, Vol. 30, 2000, pp. 183-190.
16. Kwak, Y-K., Eberhard, M., Kim, W-S., Kim, J. Shear Strength of Steel Fiber Reinforced Concrete Beams without Stirrups. *ACI Structural Journal*, July/August, No. 99-S55, 2002, pp.530-538.
17. MacDonald, C.N., and Trangsrud, J. Steel Fiber Product Introduction through Pre-Cast Reinforced Concrete Pipe. *ACI Special Publications*, Vol. 222, No. SP222-13, 2004, pp.185-198.
18. Mikhaylova, A., *Non-Linear Finite Element-Based Material Constitutive Law for Zero Slump Steel Fiber Reinforced concrete Pipe Structures*, PhD Dissertation, University of Texas at Arlington, Arlington, 2013.
19. Mohammadagha, M., *Structural and Material Performance of Rubberized and Hybrid Concrete Pipes*, MS thesis, University of Texas at Arlington, Arlington, 2013.

20. Peyvandi, A., P. Soroushian, and S. Jahangirnejad. *Enhancement of the Structural Efficiency and Performance of Concrete Pipes through Fiber Reinforcement*, Construction and Building Materials, Vol.45, 2014.
21. Products | Maccaferri Balkans. *Maccaferri Balkans Products Category*. N.p., n.d. Web. 6 May 2014. <<http://www.maccaferribalkans.com/al/category/products/>>.
22. Ramaswamy and Thomas, J, A. Mechanical Properties of Steel Fiber-Reinforced Concrete. *Journal of Materials in Civil Engineering*, May 2007, Vol. 19, Issue 5, pp. 385-392.DOI:10.1061/ (ASCE) 0899-1561(2007)19:5(385).
23. Roesler, J.R., Lange, D.A., Altoubat, S.A., Rieder, K., Ulreich, G.R. Fracture of Plain and Fiber-Reinforced Concrete Slabs under Monotonic Loading. *Journal of Materials in Civil Engineering*, Sept/Oct 2004, Vol. 16, Issue 5, pp. 452-460. DOI: 10.1061/ (ASCE) 0899-1561(2004)16:5(452).
24. Shende, A.M., and Pande, A.M. Comparative study on Steel fiber reinforced Cum control concrete under flexural and deflection. *International Journal of Applied Engineering Research, Dindigul*, 2011, Vol. 1, No. 4, pp. 942-950. ISSN-0976-4259.
25. Song, P.S., Hwang, S., Sheu, B.C. Strength properties of nylon- and polypropylene-fiber-reinforced concretes. *Cement and Concrete Research*, Vol. 35, 2005, pp. 1546-1550.
26. Swamy, R.N., and Kent, B. Some Practical Applications of Steel Fiber Reinforced Concrete. *American Concrete Institute*, Vol. 44, No. SP44-18, 1974, pp. 319-336.
27. Thomas, J., and Ramaswamy, A. Mechanical Properties of Steel Fiber-Reinforced Concrete. *Journal of Materials in Civil Engineering*, May 2007, Vol.19, Issue 5, pp. 385-392.DOI:10.1061/ (ASCE) 0899-1561(2007)19:5(385).

28. Wang. Toughness Characteristics of Synthetic Fiber-Reinforced Cementitious Composites. *Fatigue & Fracture of Engineering Materials & Structures*, April 1998, Vol. 2, Issue 4, pp.521-531.
29. Wilson, A., and Abolmaali, A., *Comparison of Material behavior Of Steel And Synthetic Fibers In Dry-cast Application*. Transportation Research Board Journal, 2013.
30. Wilson, A., *Performance Evaluation and Finite Element Analysis of Fiber Reinforced Precast Concrete Underground Structures*, MS thesis, University of Texas at Arlington, Arlington, 2012.

### Biographical Information

Sasan Farrokhi Gozachi was born in Babol, Iran, on the 10th of April,1990. He moved to Botswana, Africa, at the age of 4 and resided there until the second year of college. Upon graduating from high school, he attended the University Of Botswana in fall 2007, seeking for a Bachelor s degree in Civil engineering. After two years at the University of Botswana, he transferred to University of Texas at Arlington, and earned his Bachelors in Civil engineering in spring 2012. Later that year, fall 2012, he continued to seek for higher education, and enrolled for Masters in Civil Engineering (structures) from the University of Texas at Arlington, under the supervision of Dr. Ali Abolmaali. Sasan plans to graduate and pursue his dream of becoming a design engineer working in the industry, and becoming a professional engineer, (P.E).